Victor Prost[1]
GEAR Laboratory,
Department of Mechanical Engineering,
Massachusetts Institute of Technology,
Cambridge, MA 02139
e-mail: vprost@mit.edu

W. Brett Johnson
GEAR Laboratory,
Department of Mechanical Engineering,
Massachusetts Institute of Technology,
Cambridge, MA 02139
e-mail: wbrettjohnson@gmail.com

Jenny A. Kent
Department of Integrated Health Sciences,
University of Nevada,
Las Vegas, NV 89154
e-mail: jenny.kent@unlv.edu

Matthew J. Major
Department of Physical Medicine and Rehabilitation,
Northwestern University,
Jesse Brown VA Medical Center,
Chicago, IL 60611;
Department of Biomedical Engineering,
Northwestern University,
Jesse Brown VA Medical Center,
Chicago, IL 60611
e-mail: matthew-major@northwestern.edu

Amos G. Winter, V[1]
GEAR Laboratory,
Department of Mechanical Engineering,
Massachusetts Institute of Technology,
Cambridge, MA 02139
e-mail: awinter@mit.edu

Systematic Assessment of Prosthesis Stiffness on User Biomechanics Using the Lower Leg Trajectory Error Framework and Its Implication for the Design and Evaluation of Ankle-Foot Prostheses

Advances in understanding the effects the mechanical characteristics of prosthetic feet on user biomechanics have enabled passive prostheses to improve the walking pattern of people with lower limb amputation. However, there is no consensus on the design methodology and criteria required to maximize specific user outcomes and fully restore their mobility. The Lower Leg Trajectory Error (LLTE) framework is a novel design methodology based on the replication of lower leg dynamics. The LLTE value evaluates how closely a prosthetic foot replicates a target walking pattern. Designing a prosthesis that minimizes the LLTE value, optimizes its mechanical function to enable users to best replicate the target lower leg trajectory. Here, we conducted a systematic sensitivity investigation of LLTE-optimized prostheses. Five people with unilateral transtibial amputation walked overground at self-selected speeds using five prototype energy storage and return feet with varying LLTE values. The prototypes' LLTE values were varied by changing the stiffness of the participant's LLTE-optimized design by 60%, 80%, 120%, and 167%. Users most closely replicated the target able-bodied walking pattern with the LLTE-optimized stiffness, experimentally demonstrating that the predicted optimum was a true optimum. Additionally, the predicted LLTE values were correlated to the user's ability to replicate the target walking pattern, user preferences, and clinical outcomes including roll-over geometries, trunk sway, prosthetic energy return, and peak push-off power. This study further validates the use of the LLTE framework as a predictive and quantitative tool for designing and evaluating prosthetic feet. [DOI: 10.1115/1.4056137]

1 Introduction

Individuals with transtibial (below-knee) amputation are restricted in their mobility due to the functional limitations of commonly prescribed prostheses that induce compensatory gait patterns [1–3]. Instead of utilizing a quantitative and predictive design methodology, the development process of commonly prescribed prosthetic feet relies on extensive user testing and iterative design improvements [3]. This limits the development of prosthetic devices that could further restore the mobility of prosthesis users [3–5]. To design prosthetic devices that restore the mobility of people with amputation, research has focused on understanding the effects of the prosthesis' mechanical characteristics on the user's walking pattern [3,6,7]. These studies have mapped mechanical characteristics of prosthetic feet to biomechanical outcomes, but mostly demonstrated the effects of individual mechanical properties, such as stiffness, damping, energy return, and roll-over geometry, on locomotion. In addition, many studies investigate mechanical properties of existing commercial feet through comparative studies [6,8–11]. While these studies give a relative understanding of the performance of, and preference toward, a given prosthetic device, they do not provide absolute design targets or objectives. The relationships between the mechanical functions of prosthetic feet and user outcomes have yet to be fully understood [8]. As a result, there is a lack of quantitative design criteria required to maximize specific user outcomes [3–7,12], and prosthetic device development instead relies on user testing to iteratively design and validate products. Without a quantitative and predictive prosthetic foot design methodology that would facilitate the development of novel prosthetic feet, there is a lack of prostheses developed and designed to specifically meet a user's individual characteristics (body mass and size), needs, and target walking patterns [3,6,13].

The Lower Leg Trajectory Error (LLTE) framework [14,15] is a novel approach that enables the design and evaluation of user-specific prostheses by quantitatively and predictively connecting the mechanical characteristics of a prosthetic foot to the gait of individuals with an amputation. It differs from the traditional rationale of minimizing metabolic cost in locomotion [16,17] as sufficient evidence has suggested that humans do not optimize gait according to metabolic cost alone, especially for prosthesis users who can also be concerned with stability, kinematic appearance, functionality, symmetry, social acceptance, and long term injury [3,17,18].

The LLTE framework considers the mechanics of prosthetic feet from the standpoint of the user's lower leg, modeling the

[1]Corresponding authors.

Manuscript received February 7, 2022; final manuscript received October 21, 2022; published online December 5, 2022. Assoc. Editor: Bruce MacWilliams.

prosthetic foot as a black box and allowing for a wide range of prosthetic foot architectures. It focuses on the replication of functional characteristics rather than individual properties, or the form of the ankle-foot system. It aggregates all of the prosthetic foot's individual mechanical properties, such as roll-over geometry, stiffness, and energy storage and returns, into a single methodology that evaluates the biomechanical function of the prosthesis. One assumption behind the LLTE framework is that by designing prostheses that closely replicate able-bodied walking patterns, these devices will be valued by prosthesis users [3,17] and encourage secondary walking benefits such as symmetry, increased energy return, improved balance or reduced intact limb loading [14]. This approach of quantitatively and predictively designing prosthetic feet by modeling the user's lower leg is of growing interest [19–21], as it is agnostic of any foot architectures, facilitates the development and evaluation of prosthetic devices, allows designers to meet cost and manufacturing requirements, and departs from iterative design methodologies that rely on extensive user testing.

The LLTE framework enables the systematic tuning of the mechanical properties of passive prosthetic feet (geometry and stiffness) to yield a desired biomechanical response [22]. For a given user, a reference walking dataset is scaled to the person's body characteristics (mass, height, and foot length): the walking loads and ground reaction forces (GRFs), are scaled by the user's body mass; the location where these loads are applied on the foot, the center of pressure (CoP) locations, are scaled by the user's foot length; and the walking kinematics, joint trajectories, are scaled by the user's body size. The framework then uses a constitutive model of the prosthetic foot to calculate the prosthetic side lower leg trajectory over stance, defined as the walking phase during which the foot is in contact with the ground. For each instance of stance, the target reference GRF at a specific CoP is applied to the prosthetic foot. The resulting deformed shape of the prosthetic foot is then used to compute the lower leg orientation and position (Fig. 1).

The LLTE is a single-value objective that represents the deviation (i.e error) between the calculated prosthetic side lower leg trajectory with that of the target reference lower leg trajectory throughout a step. The LLTE is defined as

$$\mathrm{LLTE} = \left[\frac{1}{\mathrm{N}}\sum_{\mathrm{n}=1}^{\mathrm{N}}\left\{\left(\frac{x_{\mathrm{knee,n}}^{\mathrm{model}} - x_{\mathrm{knee,n}}^{\mathrm{ref}}}{\bar{x}_{\mathrm{knee}}^{\mathrm{ref}}}\right)^2 + \left(\frac{y_{\mathrm{knee,n}}^{\mathrm{model}} - y_{\mathrm{knee,n}}^{\mathrm{ref}}}{\bar{y}_{\mathrm{knee}}^{\mathrm{ref}}}\right)^2 + \left(\frac{\theta_{\mathrm{LL,n}}^{\mathrm{model}} - \theta_{\mathrm{LL,n}}^{\mathrm{ref}}}{\bar{\theta}_{\mathrm{LL}}^{\mathrm{ref}}}\right)^2\right\}\right]^{\frac{1}{2}} \tag{1}$$

where the superscripts "model" and "ref" refer to values calculated by the constitutive model and values from the reference dataset, respectively. N is the total number of frames (time instances for which the walking data is captured) included in the calculation, with n indicating each individual frame. The knee coordinates and lower leg orientation deviations are normalized by the mean of each reference variable across the considered walking frames (notated by $\bar{x}_{\mathrm{knee}}^{\mathrm{ref}}$ for the knee horizontal coordinate, for example). The LLTE framework consists of using the LLTE value as an optimization metric, and varying the prosthetic foot's mechanical characteristics to minimize the foot's LLTE value while satisfying prescribed stress constraints [14,15]. The resulting LLTE-optimized foot design enables the user to closely replicate the target lower leg kinematic and kinetic data [15]; the lower the LLTE value, the closer the replication of the target walking pattern.

The LLTE metric has shown promise as a single-value objective capable of characterizing the biomechanical behavior of experimental prosthetic feet throughout a step [23,24]. Recent work used the LLTE framework to design customized, mass-manufacturable, low-cost, Nylon 6/6, energy storage and return (ESR) prostheses to replicate able-bodied level-ground walking at comfortable speed [15,22,25]. In a gait study involving five transtibial prosthesis users, these LLTE-optimized prosthetic feet were tested against a standard commercially available carbon fiber ESR foot as well as the participants' daily-use prosthesis. The LLTE feet enabled closer replication of the target able-bodied lower leg kinematics and kinetics compared to the standard ESR foot as well as an increase in energy return, center of mass (COM) propulsion work and peak foot push-off power compared to both the standard ESR feet and daily-use feet [15,26]. A ruggedized version of these LLTE feet with a cosmetic cover was used by 16 transtibial prosthesis users over five months in a field trial in India [26,27]. The ruggedized LLTE feet showed minimal wear and degradation and enabled users to increase their walking speed on level ground [26,27]. In addition, ESR feet have been developed using the LLTE framework and tested to withstand ISO 10328 standards [25]. These results support the use of the LLTE framework to design customized prosthetic feet that replicate a target walking pattern.

Despite these initial results, the effects of changes in LLTE values on the lower leg dynamics and traditional biomechanical measures such as prosthetic foot push-off power, returned energy, peak limb loading, and roll-over geometries have not been explored. Understanding the effects of varying LLTE values on walking performance and user outcomes would provide information on the sensitivity of the LLTE-optimized designs, and further facilitate decisions on design tradeoffs and sizing of prosthetic feet by designers.

The objective of this work is to systematically explore the effects of prosthetic feet with varied LLTE values on users' walking dynamics to evaluate the sensitivity and effectiveness of LLTE-optimized foot designs. By exploring the effects of prosthetic feet with varying LLTE values on users' walking dynamics, we aim to verify that prosthetic feet with lower LLTE values enable a closer replication of the target lower leg kinematic and kinetic data compared to prosthetic feet with higher LLTE values. Then, we aim to quantify the sensitivity toward the LLTE-optimized feet by evaluating the extent to which variations in LLTE value and foot stiffness affect walking performance and

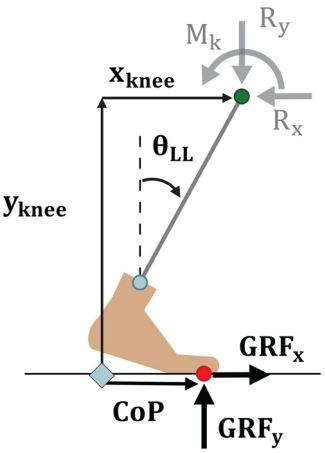

Fig. 1 Schematic of the LLTE design framework with the force and moment balance analysis conducted on the lower leg system in the sagittal plane. The position of the lower leg segment is defined by the horizontal and vertical positions of the knee (x_{knee} and y_{knee}), and the angle of the lower leg (θ_{LL}). Under prescribed loading conditions (CoP, GRF_x, and GRF_y) these coordinates can be calculated from the prosthetic foot model deformations. The orientation of the lower leg affects not only the gait kinematics of the user, but also the reaction loads at the knee (R_x, R_y, and M_k).

user outcomes. In addition to guiding the design of prosthetic feet, the validation of the LLTE metric's sensitivity may inform the prescription process by providing a comprehensive amputee-independent measure for selecting an appropriate set of prosthetic devices for specific target user outcomes and walking activity.

2 Experimental Methods

2.1 Designing Feet With Varying Lower Leg Trajectory Error Values. To investigate the effect of a foot's LLTE value on the level ground walking performance of a prosthesis user, the LLTE design framework was used to create a set of ESR foot prototypes with varying predicted LLTE values. Single-part ESR foot prototypes made of Nylon 6/6 were designed specifically for this study based on a parametric single-keel foot architecture developed in previous work (Fig. 2) [15,22,25]. The parametric single-keel foot shape was chosen for its simplicity, ease of manufacturing, and mechanically and clinically validated behavior [15,22,24,25]. Nylon 6/6 was chosen for these prostheses for its low-cost, high strain-energy density ($u \simeq 2.4\,10^3$ J/kg), and ease of machining. Its material characteristics were incorporated in the LLTE framework with a tensile modulus $E = 2.51$ GPa, tensile yield stress $\sigma_y = 82.7$ MPa, flexural modulus $E_f = 3.15$ GPa, flexural yield stress $\sigma_{yf} = 92.0$ MPa, poisson ratio $\nu = 0.41$, and density $\rho = 1130\,\text{kg/m}^3$.

The single-keel foot architecture is described using a set of wide Bézier curves (Fig. 2(*a*)) [15,22]. This parametric model defines the foot geometry and stiffness using seven control circles. The location of the control circles C_{ix}, C_{iy} defines the geometry, and the diameter of the control circles C_{id} defines the beam thickness and thus the foot stiffness. This parametrization reduces the description of complex foot geometries and stiffnesses to a limited set of design variables.

Published able-bodied level ground walking data from D.A. Winter [28] was chosen as the target reference data. There is no obviously better choice for the target reference walking dataset to use in the LLTE framework than able-bodied data, as our aims for prosthetic foot devices are to restore the biological function of the ankle and enable able-bodied walking patterns. In addition, this reference dataset allowed us to ensure that the experimental foot prototypes and LLTE framework calculations aligned with our previously clinically tested prosthetic feet designed using the LLTE framework [15,22,24].

For each study participant, an LLTE-optimized Nylon 6/6 single-keel prosthetic foot was first designed for level ground walking using the LLTE framework, as described in Sec. 1 and as an optimization formulation detailed Prost et al. [15]. For a given participant, the wide Bézier control variables were varied to minimize the LLTE value while constraining the maximum stress level to remain 40% below the Nylon 6/6 yield strength to avoid any mechanical failure during testing. The optimization problem was solved using MATLAB's (Mathworks, Natick) built-in genetic algorithm resulting in a single-part ESR foot with a specific geometry and stiffness that minimized the LLTE value for that participant.

To explore the sensitivity of the LLTE design variable and understand how prostheses with different LLTE values affect walking performance (Fig. 3), four additional prototypes were created for each participant. These prototypes were based on the geometry of the LLTE-optimized foot, but the overall prosthesis' beam bending stiffness was varied to create a range of foot designs with different LLTE values. The foot's stiffness was chosen as the mechanical characteristic to vary because it has a major effect on gait dynamics and user preference [6,29]. In addition, commercially available prostheses' stiffnesses vary across foot model, activity level, and category [30]. Systematically varying the stiffness of our prototypes enabled us to represent the range of devices used in clinical practice and previous clinical studies on foot stiffness [6,29,31].

The beam bending stiffness of the prototype feet was varied by changing the thickness of the prosthetic foot structural beam (Fig. 3(*b*)). The thickness changes were implemented by linearly changing the wide Bézier control circle diameters (Fig. 2(*a*)) that control the thickness of the foot along its geometry. The beam bending stiffness is defined as $E_{\text{nylon}}I = \frac{1}{12}E_{\text{nylon}}t^3w$, with E_{nylon} as the flexural modulus of Nylon 6/6, I as the second moment of area, t as the beam thickness along the foot, and w as the width of the foot. Changing the overall foot stiffness by a factor α required a change in the beam thickness by a factor of $\alpha^{1/3}$.

The four additional prototypes had stiffnesses of 60%, 80%, 120%, and 167% of the LLTE-optimized foot stiffness. The resulting set of five prototype prosthetic feet for a representative participant from the gait study is shown in Fig. 3(*c*). These five prototypes were labeled condition A-E in order of increasing stiffness, where condition C represents the LLTE-optimized condition. The stiffness for condition B and D were chosen to be ±20% of the LLTE-optimized foot stiffness so as to be above the

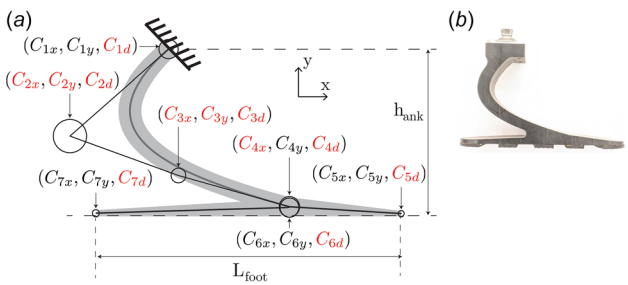

Fig. 2 Single-keel foot prototype: (*a*) parametric model defined using wide Bezier curve variables C_{ij}. The independent design variables that control the foot geometry and stiffness are shown in red (C_{1d}, C_{2x}, C_{2y}, C_{2d}, C_{3x}, C_{3y}, C_{3d}, C_{4x}, C_{4d}, C_{5d} and C_{6d}). (*b*) Manufactured single-keel foot.

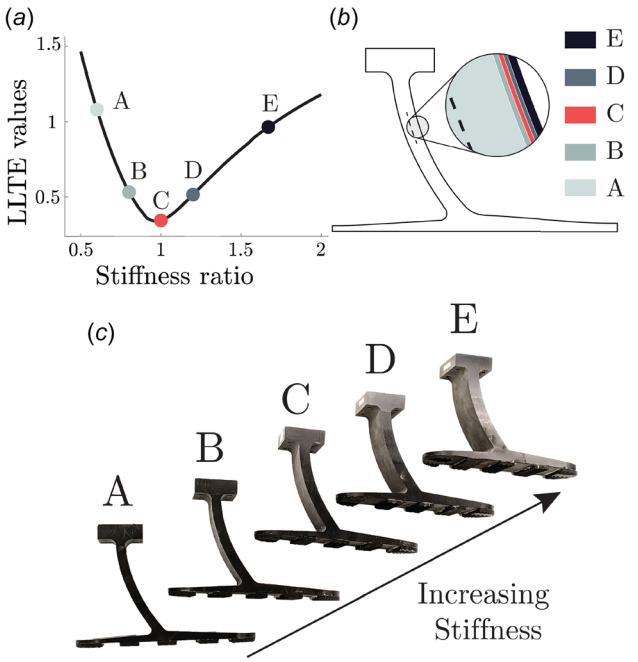

Fig. 3 Prosthetic foot prototypes labeled A-E used by participant 3 in the gait study, with A corresponding to the most compliant, E the stiffest, and C the predicted LLTE-optimized foot: (*a*) LLTE values and stiffness ratio for each prosthetic foot condition, (*b*) beam thickness variation that resulted in the stiffness change for each foot prototype. The dashed line represents the beam section neutral axis, and (*c*) photographs of the manufactured prototype feet.

Table 1 Experimental prosthetic foot prototypes' modeled trajectories using the LLTE framework for participant number 3 of the gait study

	Condition A	Condition B	Condition C	Condition D	Condition E
	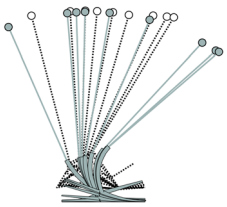	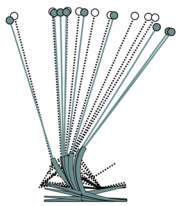	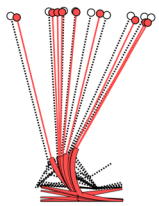	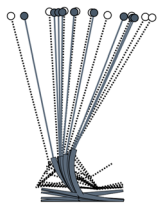	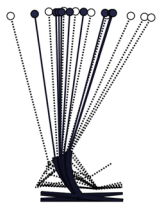
Relative stiffness	60%	80%	100%	120%	167%
LLTE value	1.080	0.531	0.325	0.515	0.965

The solid lines represent the modeled trajectories and the dashed lines the target reference trajectory.
For each foot prototype, the corresponding LLTE values and relative stiffness to the LLTE-optimized foot design, labeled condition C, are shown.

minimum perceivable stiffness change by prosthesis users [29] and similar to the stiffness change between different foot categories of commercial prostheses that a user might experience during the fitting process [32]. The stiffnesses for conditions A and E were chosen to represent the stiffness range of commercially available prosthetic feet across a range of foot types and models [31]. This set of five-foot prototypes was aimed to represent the stiffness range the user would experience during the clinical fitting and prosthesis selection process.

The LLTE framework was used to calculate the LLTE value, and modeled lower leg trajectory of each prototype. The LLTE values and the modeled lower leg trajectories, calculated from the deformed shape of the foot prototype during a step, are shown in Table 1 for a representative participant from this study. In conditions A and E, the most compliant and stiff conditions, it is not expected that the user will exhibit these extreme lower leg trajectories. In previous clinical studies, with foot prototypes designed using the LLTE framework [24], participants compensated their gait and deviated from the reference walking foot loading data instead of adopting the modeled extreme kinematics. We expected that in this study, participants would also change the loading on the prosthetic feet to avoid displaying such lower leg trajectories. The modeled lower leg trajectories for these higher LLTE values (foot conditions A and E) only provide insight into the expected increase in gait deviations from the target lower leg dynamics. The greater the deviation from the minimum LLTE value, the more gait deviation and compensation are expected by the user. The modeled lower leg trajectories for the foot condition C (the LLTE-optimized condition) is the only foot condition for which the LLTE framework has full predictive capabilities, as it minimizes the LLTE value, meaning that we would expect it to enable close-to-the target lower leg kinematics when subjected to the reference kinetics.

2.2 Study Participants. Five people with unilateral transtibial amputation (77.5 ± 25.6 kg, 1.70 ± 0.14 m, 50 ± 10.8 y/o, 18.4 ± 11.9 years postamputation) were recruited for this study (Table 2). The experimental protocol was approved by the Jesse Brown VA Medical Center Institutional Review Board, (Chicago, IL) and the Committee on the Use of Humans as Experimental Subjects at the Massachusetts Institute of Technology, (Cambridge, MA). Inclusion criteria included having a unilateral transtibial amputation and at least one year of experience walking with a prosthesis, being classified as Medicare Functional Classification Level K3 or above, and having the ability to walk for 30 min without undue fatigue or health risks. Exclusion criteria included having a body-mass index greater than 30 and comorbidities or any pathologies (other than amputation) that would affect the intact limb, the participant's balance, or stability. Participants provided informed written consent prior to data collection.

2.3 Manufactured Prototype Feet. For each one of the five study participants, a set of five Nylon 6/6 customized LLTE feet with varying LLTE values and stiffnesses were designed using the participant's body mass, lower leg length, and foot length, as described in Sec. 2.1. The LLTE-optimized foot, condition C, had varied geometries and stiffnesses across the study participants (Table 2). All 25 prototype feet were machined from Nylon 6/6 blocks using waterjet and milling machines, and fitted with a male pyramid adaptor and rubber threads for walking tests. The LLTE-optimized foot mass for each participant is listed in Table 2. Foot condition A was on average 32 ± 6.4 g, $7.8 \pm 0.9\%$ lighter than condition C, while condition E was on average 51 ± 8.9 g, $12.3 \pm 2.1\%$ heavier than condition C. Studies on the effect of foot mass on gait dynamics have shown that these changes in foot mass should have minimal effect on the user walking pattern [33,34].

Table 2 Recruited participants' characteristics and their manufactured LLTE-optimized prosthetic foot (condition C)

	Participant 1	Participant 2	Participant 3	Participant 4	Participant 5
					
Age	43	60	43	45	59
Mass	79.6 kg	89.5 kg	52.4 kg	104.0 kg	61.0 kg
Height	1.57 m	1.64 m	1.69 m	1.88 m	1.70 m
Lower leg length	0.454 m	0.459 m	0.440 m	0.536 m	0.505 m
Foot length	0.261 m	0.238 m	0.260 m	0.280 m	0.265 m
Prosthesis experience	7 years	15 years	16 years	33 years	21 years
Etiology	Dysvascular	Dysvascular	Traumatic	Traumatic	Traumatic
Prototype foot mass	0.396 g	0.387 g	0.384 g	0.469 g	0.423 g

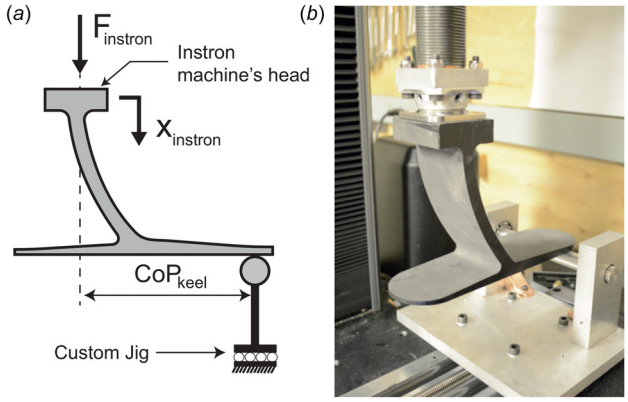

Fig. 4 Prosthetic foot mechanical tests experimental setup that includes a custom jig mounted on an Instron machine to apply normal loads on the foot at specific CoP locations: (*a*) schematic of the experimental setup and (*b*) photograph of a prototype prosthetic foot being loaded on the Instron machine

2.4 Mechanical Testing of Prototype Feet Stiffnesses. To validate the LLTE framework's constitutive model and the experimental prototype feet mechanical behaviors, static mechanical tests [15,25] were conducted using an Instron load testing machine (Instron Inc, Norwood, MA) (Fig. 4). The measured load–displacement curves were used to calculate each foot's stiffness and ensure that the constitutive model accurately predicted its performance.

The experimental setup (Fig. 4) consisted of a jig that loaded the test foot to approximately the user's body weight ($F \simeq mg$, with m equal to the mass of the user). Loads were applied at two representative locations along the plantar foot, $CoP_{keel} = 130 \pm 0.1$ mm and $CoP_{heel} = -30 \pm 0.1$ mm, measured anterior and posterior from the prosthesis ankle, respectively (Fig. 4(*a*)). The foot was loaded at a constant displacement rate of 300 mm/min. The vertical load ($F_{instron}$) and displacement ($x_{instron}$) were recorded at a rate of 10 Hz (Fig. 4(*a*)). The load cell is resistant to off-axis loading errors, with a rated maximum force measurement error of 6.4% in this setup. The displacement was measured with a rated error of ± 0.1 mm. The custom jig fixed on the Instron machine is composed of a linear stage on which an aluminum rod is mounted on a set of roller bearings to minimize friction. This rod ensures that the applied load remains normal to the foot and can be applied at specific CoPs along the foot (Fig. 4).

The experimental setup's loading conditions (heel and keel loading) were replicated using the LLTE framework's constitutive model for each prototype test foot. The normal load was applied on the foot model at the two specific CoP locations, similar to the mechanical test, and the simulated prosthetic foot deformations were recorded. The simulated load–displacement data using the constitutive model were then compared to the measured Instron values to validate the mechanical behaviors of the foot prototypes and the expected stiffness variation between the foot conditions.

2.5 Gait Study Protocol. Participants walked over level ground at their self-selected speeds with the five customized foot conditions in a randomized order. Participants were blinded to the foot condition to avoid any biases. All foot conditions were tested in a single-day session to avoid interday measurement variability [35] while allowing for as much accommodation and resting time as needed. For all conditions, participants used their own customary prosthetic socket and suspension system. The prosthetic feet were worn without a shoe to most closely match the foot model used in the LLTE framework. Each participant wore the same model of laboratory-supplied flat shoe (Mossi Damien, Mossimo Supply Co., New York, NY) on the intact side to control for and minimize the effect of footwear on stance-phase mechanics [36]. The standard alignment was performed with prosthetic foot condition C and was kept unchanged for the remaining foot conditions, as the foot geometry was identical between foot conditions for each participant (only stiffness was varied between foot conditions). In addition, maintaining the same alignment for each foot condition was necessary to avoid confounding factors, since prosthesis alignment can have a considerable effect on the user's walking mechanics [37]. The same certified prosthetist performed all modifications and alignments. Participants were then given time to accommodate each prosthetic foot condition until they verbally expressed confidence to start the walking trial.

Reflective markers were fixed to anatomical landmarks on the participant according to a modified Helen Hayes marker set [38,39]. Markers on the prosthetic foot were placed on the pyramid mount, heel, forefoot, and toe. A digital motion capture system (Motion Analysis Corporation, Santa Rosa, CA) collected kinematic data at 120 Hz. Six floor-embedded force plates (Advanced Mechanical Technology, Inc., Watertown, MA) collected kinetic data at 960 Hz. Participants were instructed to walk back and forth along a 10 m walkway at a self-selected comfortable speed. Data from a step were recorded only if the participant's entire foot landed on a single force plate, and the opposite foot did not contact that same force plate. After at least five steps were collected on each side, the participant's feedback on the prosthesis was recorded following the questionnaire described below in Sec. 2.7, before changing the prosthetic foot condition. This protocol was repeated for each foot condition after a resting and acclimation period.

2.6 Biomechanical Data Analysis. Fourth-order bidirectional 6 Hz and 12 Hz low-pass Butterworth filters were applied to the kinematic and kinetic data, respectively. The biomechanical data were then exported to MATLAB to build the limb segment model. A 40 N vertical GRF threshold was used to detect ground contact and define the stance phase. Data from each step were represented as percent of the stance phase to account for variations in walking speeds and stance time. For each biomechanical measure, the data were averaged to create a representative step for each participant, foot condition, and for both the prosthetic and intact leg. In addition, data were averaged across participants per leg and condition to create group averages after normalizing kinetic data using participant's body weight and foot size, and kinematic data using the participant's lower leg length to account for the participant's varying body characteristics [40].

Deviations *From* the Target Lower Leg Kinematics and Kinetics. To evaluate how closely each prosthetic foot enabled replication of the target able-bodied walking pattern during walking trials, we computed the normalized root mean squared error (NRMSE) between the measured and target reference lower leg kinematic and kinetic data (Fig. 5(*a*)) for both the prosthetic and intact legs over the entire stance phase. These deviation measures from the reference target dataset were grouped into six scores for each leg: GRF deviations (vertical and fore-aft, normalized (divided) by body weight), CoP progression deviation (normalized (divided) by foot length), and lower leg kinematic deviations (x_{knee} and y_{knee}, and θ_{LL} in the sagittal plane, normalized (divided) by lower leg length and reference θ_{LL} range, respectively).

To evaluate the effectiveness of each prosthesis in replicating the reference target biomechanical response, a single deviation measure was derived for each participant and for each prosthetic foot condition by summing the kinetic (GRF and CoP) and kinematic (lower leg position and orientation) deviations for both the prosthetic and intact legs (Fig. 5(*b*)). Both legs were considered in our deviation calculation since compensatory motions and loading are usually exhibited on both sides for people with unilateral amputation [41–44]. This single deviation measure for each prosthetic foot condition represents the deviations due to changes in the prosthetic foot condition as well as the deviations due to the participant's general walking ability (Fig. 5(*c*)). To aggregate and

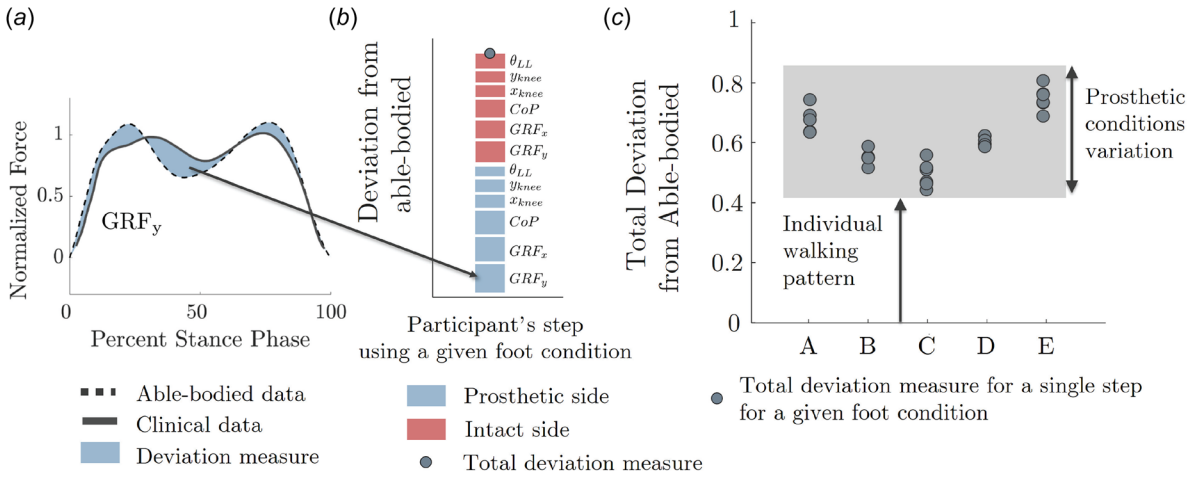

Fig. 5 Deviation measure calculation methodology. (*a*) Vertical GRF deviation from the able-bodied reference calculation using the NRMSE. (*b*) Schematic of the total deviation measure for a single step for a participant using a given prosthetic foot. The total deviation measure is calculated as the summed deviation measures of each metric and each leg. (*c*) Total deviation measure for each step and prosthetic foot condition for a representative participant. It represents both the participant's general walking ability and changes due to the various foot conditions.

evaluate the effects across all the participants due only to prosthetic foot conditions (stiffness variations) and not due to the participants' general abilities to walk, the deviation measures for each foot condition were normalized by that of condition C, the LLTE-optimized condition. In the aggregated data, the normalized deviation measure for a given foot condition for a given participant was calculated by taking ratio of the total deviation measure (Fig. 5) by the total deviation measure from foot condition C. This normalization results in the deviation measure for condition C to be centered around 1 for each participant, enabling a comparison across each participant of the relative effects of varying prosthetic foot conditions from the defined optimal foot condition C on the user gait pattern.

Kinematic Gait Parameters. For each individual step, the following metrics were calculated to evaluate the effects of each prosthetic foot condition on the participant's walking dynamics: walking speed, Froude number (Fr) [45], stance time symmetry index [46], step width [47], trunk sway angle [48], and prosthetic foot angle [49]. The walking speed was calculated as the average speed of the sacrum marker in the direction of travel over a single trial. To account for the different participants' body sizes, Froude numbers were also calculated as $Fr = v^2/gL$ with v the walking speed and L the participant's leg length, measured from the hip (greater trochanter) to the floor [45]. The stance phase symmetry index (SI) [46] was defined as $\mathrm{SI} = 100(1 - \frac{|X_P - X_S|}{0.5|X_P + X_S|})$, with X_P and X_S representing the prosthetic and intact side stance times, respectively, and 100% corresponding to perfect symmetry. The trunk reference frame was defined using the two shoulder markers and the sacrum marker. The lateral trunk sway angle was then calculated from the trunk reference frame motion in the participant's frontal plane relative to the lab reference frame [48]. The step width was calculated as the average medial-lateral distance between the ankle joint centers at each foot-ground contact [47]. ESR prosthetic feet are designed to deform in order to store and return energy. The deformation of these compliant structures makes it difficult to define the rotation of the foot segment about the shank segment as a single-axis rotation. To overcome this limitation, the prosthetic foot angle was defined as the projection in the sagittal plane of the angle between the foot segment, defined by the heel, lateral ankle, and toe markers, and the shank segment, defined by the shank, lateral ankle, and lateral knee markers [49]. The foot neutral angle was then calculated during the swing phase of the gait cycle when no forces were applied to the prostheses.

Kinetic Gait Parameters. Roll-over shape radius, effective foot length ratio (EFLR), prosthetic foot power, step-to-step transition work, ankle joint moments, foot power, and GRF peak values were calculated to evaluate the walking benefits and effects of each prosthetic foot condition. The roll-over shape radius was calculated as the radius of the arc described by the CoP from heel strike to the opposite heel strike in the shank reference frame. The effective foot length is defined as the distance from the heel to the anterior end of the roll-over shape, which corresponds to the location of the roll-over shape at the time of opposite heel contact [37]. The EFLR is then calculated as the ratio of the effective foot length and the foot length [50]. The prosthetic foot power was calculated as the distal shank power based on the unified deformable segment model [51], which treats the foot as a flexible structure and calculates the power absorbed and returned distal to the shank. Since ESR prosthetic feet have no fixed ankle joint axis and violate the rigid body assumption, this methodology may be more appropriate than the traditional inverse dynamics calculations [52]. The energy stored and returned during propulsion was calculated as the time integral of the negative and positive portions of foot power during the stance phase of gait and then normalized by body mass. Step-to-step transition work was

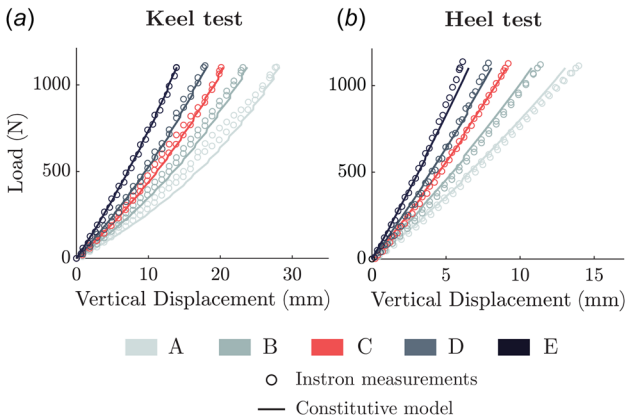

Fig. 6 Load-displacement curves of participant 4's foot conditions (A–E) measured with the Instron machine and compared to the constitutive model. (*a*) Keel loading tests at $\mathrm{CoP_{keel}} = 130 \pm 0.1$ mm. (*b*) Heel loading tests with $\mathrm{CoP_{heel}} = -30 \pm 0.1$ mm. Load displacement results for other participants are shown in Appendix A.

calculated to define how each limb contributed to the overall propulsion or collision work of the body center of mass (CoM). First, the external mechanical power generated by a limb was computed as the dot product of the limb's GRF and the velocity of the CoM. Integrating these external mechanical powers during the collision or propulsion phases resulted in the step-to-step transition work [53,54].

2.7 User Feedback. Participant feedback on each prosthetic foot was collected using a custom prosthetic foot evaluation questionnaire (see Supplemental Materials on the ASME Digital Collection) administered after completing the walking trial for each foot condition. This questionnaire captured attributes valued by people with amputation that are not captured by biomechanical analysis, such as comfort, pain, walking effort, stability, confidence, or appearance, [12,55] but assisted with results interpretation. Each answer from the questionnaire was converted into a 5-point Likert scale (1-Strongly disagree to 5-Strongly agree) and summed into a total score out of 50. This evaluation score was used to assess a participant's preference toward a prosthetic foot, with a higher score corresponding to a higher user preference.

2.8 Statistical Analysis. All scalar values such as peak force were first calculated for each step for individual participants and then averaged across steps and across participants to avoid any artifacts from averaging. Variance is represented as interparticipant standard deviation for participant-averaged data and as intersteps standard deviation for individual participants' data.

All data were determined via a Shapiro-Wilk test to be nonnormally distributed. Therefore, a Friedman's test was used as a nonparametric, repeated measures analysis of variance to assess group-level main differences between prosthetic foot conditions in all biomechanical variables and participant evaluation scores. Following this, pairwise comparisons to evaluate differences between two-foot conditions were conducted with a Wilcoxon signed test procedure with Holm-Bonferroni corrections for multiple comparisons to account for Type-1 error rates. Statistical analyses were performed in MATLAB with the critical α set at 0.05.

Given the small sample size, single-participant analyses were also performed to identify individual responses to prosthetic foot conditions. Using a published MATLAB function [56] of the Model Statistic tests, a single-participant approach described by Bates [57] was conducted for the biomechanical variables and the significance level was set for critical α values of 0.05.

3 Results

3.1 Mechanical Testing Validates the Lower Leg Trajectory Error Framework's Constitutive Model. Across all five prosthetic foot conditions for each participant and the two loading cases (heel and keel), the vertical displacements (Fig. 6) were predicted with a maximum error of 2.8 mm over deformations of 37.9 mm. The average error across all foot prototypes over the load-displacement curve was 0.6 ± 0.5 mm or $6.3 \pm 3.5\%$. The foot prototypes' stiffnesses were all measured to match the desired stiffnesses with an average error of $3.1 \pm 2.2\%$.

In addition, the average energy storage and return efficiency of these prototypes was $94.6 \pm 0.9\%$ (Fig. 6). These small efficiency losses are likely due to viscous effects in the material and supports our purely elastic behavior assumption of Nylon 6/6, as these losses did not impact the predicted deformation of the prosthetic foot prototypes. The experimental prototypes accurately replicated the desired mechanical behavior, warranting their use in the gait study.

3.2 Replication of Target Lower Leg Dynamics. All of the participants' gait patterns were affected by the changes in prosthetic foot conditions. They exhibited varying levels of deviations from the able-bodied reference walking pattern for the lower leg trajectory (x_{knee}, y_{knee}, and θ_{LL}) and loading pattern (GRF_x and GRF_y) on the prosthetic side and for the vertical GRF on the intact side (Figs. 7 and 8).

On the prosthetic side, decreasing the foot stiffness (conditions A and B) resulted in an increased knee drop-off at the end of stance, smoother CoP progression, reduced second peak in GRF_y, and increased first peak in GRF_y (Fig. 7). The reduced stiffnesses of conditions A and B compared to condition C resulted in a drop-off of the knee at the end of stance, as shown by the increased deviation from able-bodied reference for x_{knee}, y_{knee}, and θ_{LL} (Figs. 7 and 8(*a*)). In addition, the reduced stiffness from conditions A and B resulted in a lower second vertical GRF peak compared to condition C. Increasing the prosthetic foot stiffness

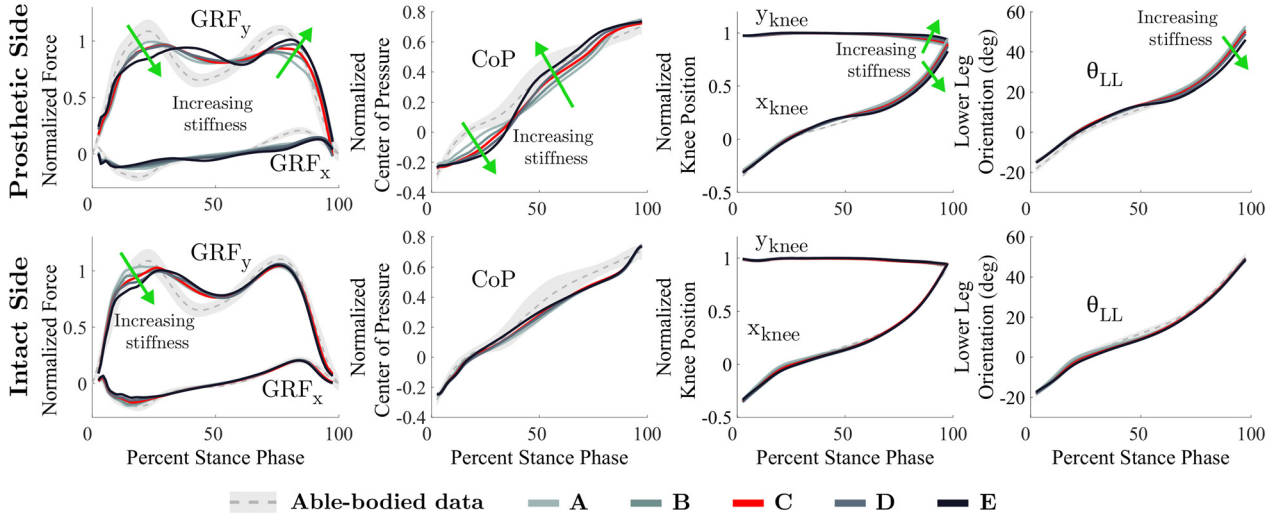

Fig. 7 Average kinetic and kinematic variables over the entire stance phase for each prosthetic foot type averaged across all participants. This includes horizontal and vertical ground reaction forces (GRF_x and GRF_y), center of pressure (CoP) progression, and lower leg position and orientation in the sagittal plane (x_{knee}, y_{knee}, and θ_{LL}). Results are shown for the both the prosthetic and intact side, and compared to the corresponding reference physiological data [28] used in the LLTE framework to optimize the foot. The shaded regions correspond to one standard deviation of the normative physiological data. The green arrows show the effects of the increasing stiffness from the tested foot conditions. Individual participant's data are provided in Appendix B.

(conditions D and E) resulted in an increased time to foot flat, reduced GRF_y first peak, and a lower leg angle at the end of stance (Figs. 7 and 8(*a*)). The increased stiffness at the heel resulted in a reduced loading rate on the prosthetic leg, as shown by the depressed first GRF_y peak, and increased time to foot flat with the CoP remaining at the heel of the foot before quickly transitioning to the toes around midstance. This abrupt CoP progression and the changes in vertical loading resulted in increased deviation from able-bodied for the CoP and GRF_y when compared to condition C (Fig. 8(*a*)). Similarly, the increase in stiffness resulted in a reduced lower leg angle and knee progression at the end of stance compared to able-bodied. Condition C, the LLTE-optimized prosthesis, was the only foot condition that led to a smooth CoP progression, prevented drop-off at the end of stance, and ensured a closer replication of the GRF_y profile compared to the other conditions.

At a group level, the LLTE-optimized feet (condition C) enabled a closer replication of the target able-bodied walking profile compared to the remaining conditions, aligning with the lower LLTE value for condition C compared to the other foot conditions (Fig. 8). Condition C resulted in the least deviation from the able-bodied target lower leg dynamics compared to the other conditions and produced values that were significantly lower than those of conditions A, D, and E (Fig. 8(*b*)). When using prosthetic feet with higher predicted LLTE values, participants exhibited increased deviations. This is shown by the quadratic trend, centered around condition C ($R^2 = 0.514$, $p < 0.001$), of the total deviations from able-bodied data (Fig. 8(*b*)). Condition C resulted in a total averaged deviation from able-bodied lower leg biomechanics that was 6.3% ($p = 0.032$) lower than condition A, 2.9% ($p = 0.346$) lower than condition B, 6.9% ($p = 0.030$) lower than condition D, and 17.7% ($p < 0.001$) lower than condition E. At an individual level, four out of the five participants exhibited the same quadratic trend in the total deviation from able-bodied, with condition C resulting in the lowest deviations compared to the remaining conditions (Fig. 8(*b*)). For participants 1 and 3, condition C resulted in significantly lower deviations compared to the remaining conditions. For participants 4 and 5, deviations for condition C were significantly lower compared to conditions A, D, and E but not B. On the contrary, participant 2 exhibited a highly variable walking pattern and did not display the similar quadratic trend in which condition C resulted in significantly lower deviation than the remaining conditions, except when compared to condition E, the stiffest condition (Fig. 8(*b*)). For participant 2 while the lowest deviation was displayed using foot condition D, the difference with condition C was not significant. Changes in prosthetic foot condition had little effect on participant 2. Individual participants' GRFs, CoP, and lower leg kinematics are provided in Appendix B.

Changes in prosthetic foot conditions did not result in differences in the intact side lower leg trajectory or CoP progression and instead only impacted the first peak of the vertical and horizontal GRFs (Figs. 7 and 8(*a*)). Prosthetic foot conditions had a larger effect on the prosthetic side lower leg kinetics than the kinematics. The deviations from able-bodied were on average ~ 3.3 times lower on the lower leg trajectory compared to deviations in foot loading, suggesting that the participants in this study walked in such a way as to maintain close-to able-bodied kinematics regardless of the foot condition they were given.

3.3 Gait Parameters. Changes in foot condition were illustrated by the variations in the prosthetic foot peak dorsiflexion and plantarflexion angles among all participants (Table 3). Prosthetic foot peak dorsiflexion and plantarflexion angles decreased with the stiffness of the foot conditions A-E ($p < 0.001$ and $p < 0.001$), with A the most compliant condition and E the stiffest. The ranges of motion of the prosthetic feet across all participants were 23.3 ± 3.2 deg for condition A, 20.4 ± 3.1 deg for condition B, 17.7 ± 1.7 deg for condition C, 16.0 ± 2.6 deg for condition D,

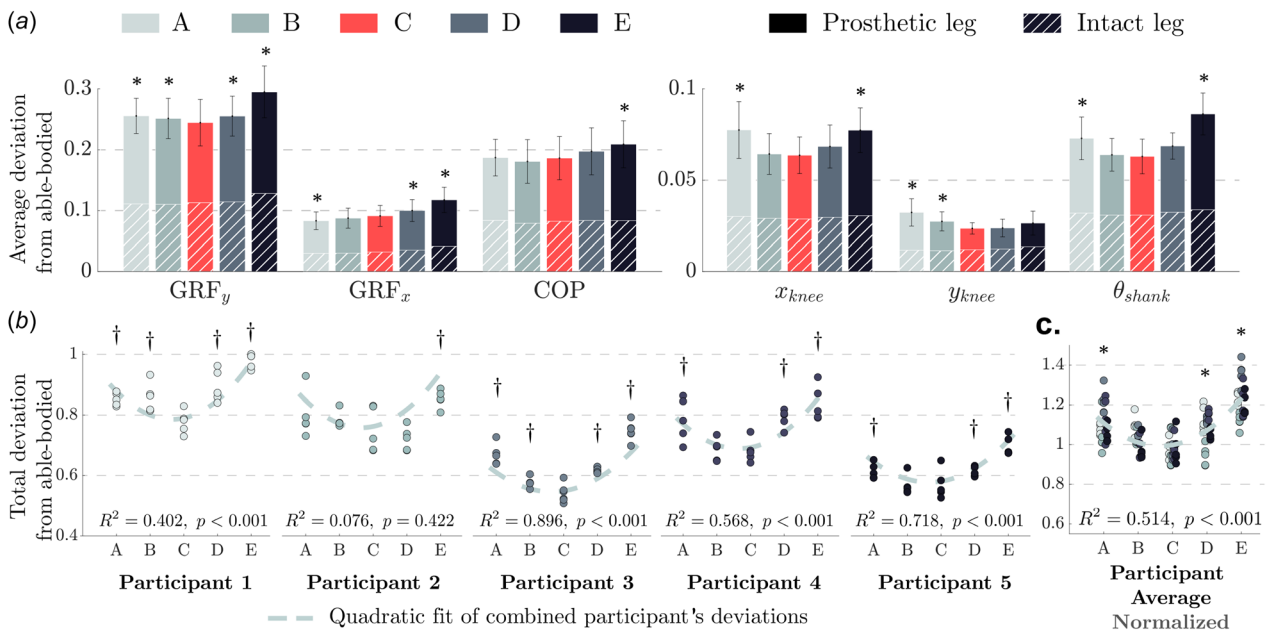

Fig. 8 Measured deviations from the able-bodied reference data for all prosthetic foot conditions and study participants. (*a*) Average deviation for all participants across the lower leg kinematic and kinetic variables for both prosthetic and intact legs. The deviation resulting from the intact leg is shown with a hatched pattern. (*b*) Total deviation, summed from all six kinematic and kinetic variables, is shown for each participant and foot condition. Each circular marker represents the total deviation from a single step, while the marker colors represent the different participants. The dashed line is the quadratic fit of the normalized total deviation from the participant average. (*c*) Total deviation for the participant average which was normalized about condition C to only show the changes due to foot condition variations as described in Sec. 2.6. Group level statistical significant pairwise difference between the starred foot condition and foot condition C shown with *, and individual statistical significant pairwise difference is shown with †.

Table 3 Gait parameters for the five prosthetic foot conditions labeled A-E during over-ground walking at self-selected speeds

Measure	Condition A	Condition B	Condition C	Condition D	Condition E
Kinematic					
Walking speed [m/s]	1.23 ± 0.08	1.23 ± 0.13	1.25 ± 0.13	1.26 ± 0.11	1.19 ± 0.15*
Froude number	0.18 ± 0.02	0.18 ± 0.03	0.19 ± 0.03	0.19 ± 0.03	0.17 ± 0.04*
Stance time symmetry	94.5 ± 4.7	93.8 ± 6.1	93.6 ± 5.2	93.8 ± 5.2	92.6 ± 5.4
Step width [m]	0.13 ± 0.03	0.12 ± 0.03	0.12 ± 0.03	0.12 ± 0.03	0.13 ± 0.03
Trunk sway range of motion [deg]	6.6 ± 2.5*	6.5 ± 3.0	6.1 ± 2.4	6.2 ± 2.4	6.6 ± 3.1*
Peak dorsiflexion angle [deg]	15.7 ± 2.6*	13.8 ± 2.5*	12.1 ± 2.3	11.0 ± 2.1*	8.6 ± 1.6*
Peak plantarflexion angle [deg]	7.6 ± 1.3*	6.6 ± 0.9*	5.7 ± 0.7	5.0 ± 0.7*	3.5 ± 0.8*
Kinetic					
Roll over shape radius [m/m]	0.27 ± 0.05*	0.30 ± 0.06*	0.34 ± 0.06	0.37 ± 0.05	0.47 ± 0.10*
Effective foot length ratio (EFLR) [m/m]	77 ± 13*	81 ± 12	83 ± 12	86 ± 14*	89 ± 13*
Energy returned by prosthetic foot [J/kg]	0.24 ± 0.03	0.23 ± 0.04	0.23 ± 0.03	0.21 ± 0.04*	0.16 ± 0.03*
Peak prosthetic foot push off power [W/kg]	2.6 ± 0.4	2.6 ± 0.6	2.4 ± 0.6	2.1 ± 0.7*	1.5 ± 0.5*
CoM collision work by prosthetic leg [J/kg]	0.08 ± 0.03	0.08 ± 0.03	0.07 ± 0.02	0.07 ± 0.02	0.07 ± 0.03
CoM propulsion work by prosthetic leg [J/kg]	0.15 ± 0.04*	0.17 ± 0.03	0.18 ± 0.04	0.19 ± 0.03	0.17 ± 0.04
CoM collision work by intact leg [J/kg]	0.15 ± 0.05*	0.12 ± 0.04*	0.08 ± 0.03	0.06 ± 0.03*	0.02 ± 0.02*
CoM propulsion work by intact leg [J/kg]	0.27 ± 0.05	0.29 ± 0.08	0.29 ± 0.07	0.29 ± 0.07	0.26 ± 0.07
Horizontal GRF second peak on prosthetic leg [N/N]	0.14 ± 0.02	0.14 ± 0.03	0.15 ± 0.02	0.15 ± 0.04	0.12 ± 0.04*
Vertical GRF first peak on intact leg [N/N]	1.10 ± 0.08*	1.06 ± 0.09	1.05 ± 0.08	1.04 ± 0.08	1.05 ± 0.08
Intact leg peak knee abduction moment [Nm/kg]	0.30 ± 0.07	0.31 ± 0.09	0.31 ± 0.09	0.34 ± 0.08*	0.33 ± 0.10
Intact leg peak knee flexion moment [Nm/kg]	0.68 ± 0.19*	0.58 ± 0.18	0.52 ± 0.12	0.49 ± 0.07	0.42 ± 0.05*

Values shown here are averaged across all the participants.
*Significant differences from the LLTE foot condition C are denoted by an asterisk *.

and 12.1 ± 1.9 deg for condition E. These changes in foot condition affected each participant's level ground walking gait parameters to different extents. The recorded gait parameters averaged across all participants for each foot condition are shown in Table 3.

Effect of Lower Leg Trajectory Error Foot Condition on Kinematic Parameters. Participants walked with similar self-selected walking speeds of 1.23–1.26 m/s (Fr ≃ 0.18–0.19) for conditions A-D, but displayed a slower walking speed for condition E with 1.19 ± 0.15 m/s (Fr ≃ 0.17 ± 0.04) ($p < 0.001$). Despite the change in walking speed for condition E, there were no differences in stance time symmetry ($p = 0.205$) and step width ($p = 0.172$) between the foot conditions. However, trunk sway range of motion was affected by changes in foot condition, with condition C, the LLTE-optimized condition, resulting in the lowest trunk sway range of motion of 6.1 ± 2.4 deg, which was significantly lower than those of conditions A and E ($p = 0.039$ and $p = 0.044$). Trunk sway range of motion increased as the stiffness conditions deviated further from condition C, and thus with the foot's LLTE value.

Effect of Lower Leg Trajectory Error Foot Condition on Roll-*Over* Parameters. The roll-over shape radius and EFLR were closer to the averaged able-bodied values of 0.31 m/m and 0.83 m/m, respectively [50,58], for prosthetic foot conditions B and C compared to conditions A, D, and E (Table 3). Roll-over shape radii increased with the prosthetic foot stiffness conditions ($p < 0.001$), with conditions A, B, and E deviating significantly from condition C ($p < 0.001$ for all). Similarly, EFLR increased with the prosthetic foot stiffness conditions ($p < 0.001$), with conditions A, D, and E deviating significantly from condition C ($p = 0.032$, $p = 0.027$, and $p = 0.022$). The LLTE values increased the further foot stiffness deviated from condition C, meaning that prosthetic feet with lower LLTE values more closely replicated able-bodied roll-over parameters than feet with higher LLTE values.

Effect of Lower Leg Trajectory Error Foot Condition on Mechanical Work *During* Walking. Prosthetic foot conditions A, B, and C, demonstrated greater energy return, and peak push-off power, compared to stiffer conditions, D and E (Table 3, Fig. 9). The peak push-off power and the energy returned by the prosthetic foot conditions increased with foot compliance but plateaued for conditions A, B, and C, for which there was no statistical difference ($p = 0.124$). The peak push-off power was 12% ($p = 0.038$) and 58% ($p < 0.001$) higher with condition C than with conditions D and E, respectively. Similarly, energy returned by foot condition C was 9.5% ($p = 0.043$) and 44% ($p < 0.001$) higher than by conditions D and E, respectively.

Walking patterns that reduce the CoM collision work while increasing the propulsion work are linked to more efficient walking [53,59]. Here, the CoM work during propulsion was significantly lower for condition A compared to all the other prosthetic foot conditions despite demonstrating the highest level of peak push-off power and energy return. Condition A displayed 17% lower CoM propulsion work compared to condition C ($p = 0.012$). There were no significant differences across foot conditions in the CoM work during collision performed by the prosthetic leg ($p = 0.070$) and propulsion performed by the intact leg ($p = 0.171$). However, the CoM work of the intact leg during collision decreased with increased prosthetic foot stiffness ($p < 0.001$) (Table 3).

Effect of Lower Leg Trajectory Error Foot Condition on Limb Loading. To increase comfort and reduce the risk of long-term injuries, prosthetic feet aim to reduce peak knee moment and

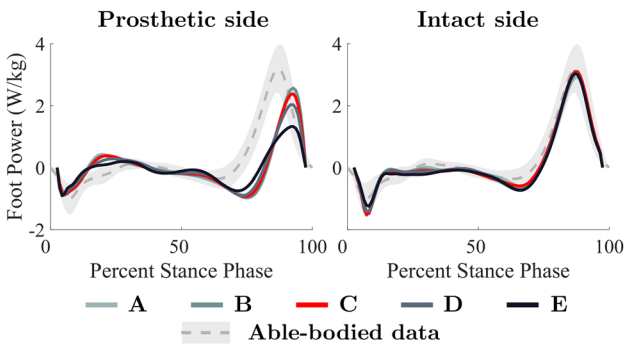

Fig. 9 Foot power over the entire stance phase for each prosthetic foot condition averaged across all participants. Results are shown for both the prosthetic and intact side, and compared to the corresponding reference physiological data [28] used in the LLTE framework. The shaded region corresponds to one standard deviation of the normative physiological data.

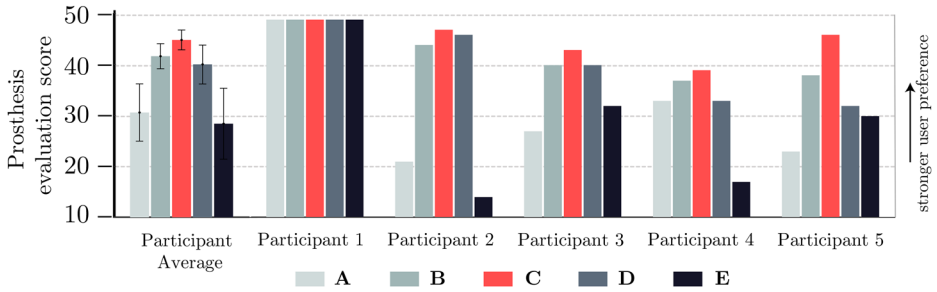

Fig. 10 Participants' prosthesis evaluation scores along with participant-averaged scores for the different prosthetic foot conditions. Higher scores are linked to stronger user preference.

vertical GRF first peak loading on the intact limb [1,60,61]. Here, more compliant prosthetic foot conditions demonstrated increased intact leg peak knee flexion moments and first vertical GRF peak loading compared to the stiffer foot conditions (Table 3). Vertical GRF first peak on the intact leg was significantly higher for condition A compared to condition C ($p = 0.048$), while the remaining conditions were not significantly different from condition C. Intact leg peak knee flexion was significantly decreased with prosthetic foot stiffness ($p < 0.001$), with condition A and E being significantly different than condition C ($p < 0.001$ and $p = 0.003$). On the contrary, intact peak knee abduction moment increased with the stiffness of the prosthetic feet, with condition D displaying a significantly higher peak knee abduction moment than condition C ($p = 0.038$).

3.4 User Feedback. The prosthesis evaluation scores for all participants and prosthetic foot conditions are shown in Fig. 10. Participant 1 scored the first prosthetic foot condition they tested (condition E) with a high, favorable score but reported preferring all the subsequent prosthetic foot conditions, making the evaluation score insensitive to changes in prosthetic foot conditions despite their dislike toward conditions D and E (Fig. 10). The remaining participants' scores varied with the prosthetic foot conditions, but they all scored condition C higher than all other conditions. Participants were all able to distinguish the different prosthetic foot conditions, the stiffness changes using "soft" or "hard", and preferred condition C to the remaining conditions, crediting increased balance and comfort, ease of walking, and the ability to walk faster. In addition, these four participants scored prosthetic foot conditions with higher LLTE values the lowest. The further the prosthetic foot stiffness varied from the LLTE-optimized condition, condition C, the lower they scored the foot. However, for participants 2, 3, and 4, the scores for condition C were only 2.2% to 6.9% higher than for conditions B and D, and their qualitative feedback stated overall comfort and ease of walking with condition C as well as conditions B and D.

4 Discussion

The goal of the LLTE metric is to provide a quantitative connection between the mechanical characteristics of a prosthetic foot and its biomechanical performance, so as to enable the evaluation and design optimization of prosthetic feet. Here, we employed a systematic approach to investigate how prosthetic feet with varying LLTE values affect the dynamics of transtibial prosthetic gait. The overall prosthetic foot stiffness was varied with respect to the LLTE-optimized stiffness to create a set of five prosthetic feet with varying LLTE values for each participant. All five participants were able to adapt and distinguish between the different prosthetic foot conditions. Results from this study suggest that the LLTE value of a prosthetic foot is correlated to its ability to enable users to replicate a target walking pattern (lower leg kinetics and kinematics) (Figs. 7 and 8), to user preferences (Fig. 10), and to clinical outcomes such as roll-over geometries, trunk sway, prosthetic energy return and peak push-off power (Table 3 and Fig. 9). Prosthetic feet with lower LLTE values best replicated the target lower leg dynamics, enabling increased walking benefits and higher user preference compared to prosthetic feet with higher LLTE values.

The LLTE-optimized prosthetic foot, condition C, enabled the closest replication of the target able-bodied lower leg kinematics and kinetics across all foot conditions (Figs. 7 and 8). In addition, the quadratic fit of the total deviation (Fig. 8) matched the quadratic shape from the prosthetic foot conditions' LLTE values (Fig. 3). The further prosthetic foot conditions deviated from condition C in terms of LLTE value and stiffness, the further the participant's walking pattern deviated from the target walking pattern.

The observed gait dynamics aligned with the insights provided by the prosthetic lower leg trajectories modeled by the LLTE framework (Table 1). Conditions A and B were predicted to be too compliant for the users (higher LLTE values compared to condition C), with excessive deformation at heel strike and toe-off (Table 1). In the measured lower leg trajectories during walking trials, the lower leg angle increased further than the able-bodied target at the end of the prosthetic side stance. The prosthetic side knee coordinates also showed a drop off, with the y-coordinate dropping lower than the target y-coordinate at the end of the stance, which suggests that the prosthetic foot conditions A and B were too compliant for the user to replicate the target able-body walking pattern (Figs. 7 and 8(*a*)). This excessive compliance would also explain the reduced prosthetic side vertical GRF second peak compared to the able-bodied target, as participants could have unloaded the prosthetic foot at terminal stance to avoid further knee drop-off from foot conditions A and B.

Similarly, conditions D and E were predicted to be too stiff for the users (higher LLTE values compared to condition C), preventing the full able-bodied lower leg range of motion during the step (Fig. 1). In the measured lower leg trajectories at the end of stance on the prosthetic side, the lower leg angle did not reach the able-bodied end of stance lower leg angle, leading to increased measured deviations as shown in Figs. 7 and 8(*a*). The excessive stiffness from conditions D and E can also be seen in the prosthetic side CoP progression, which sharply progresses from heel to toe at approximately 40% of stance instead of the smooth progression exhibited in conditions A-C. To compensate for the hard heel of these conditions and reduce the impact at heel strike, users seemed to reduce the loading on the prosthetic side (lower first vertical GRF peak). This sharp progression and hard heel led to reported discomfort and jerk in the lower leg by all the users. Condition C, the LLTE-optimized stiffness, resulted in a smooth progression of the CoP, shock absorption at heel strike, replication of the able-bodied lower leg trajectory, minimal drop-off, and the appropriate support at the end of stance, as shown by the second vertical GRF peak. The fact that condition C enabled the closest replication of the target able-bodied lower leg dynamics aligns with the estimated lower leg trajectory and minimized LLTE value from the

LLTE design framework (Table 1 and Fig. 3). These results were displayed across all participants despite the different foot geometries (Table 2), and wide range of participant's body mass and height (52.4 to 104.0 kg, and 1.57 to 1.88 m), supporting the use of the LLTE value as a design objective and predictive evaluation measure for comparing the relative stiffness and walking performance of prosthetic feet.

Across all prosthetic foot conditions, the deviations from the able-bodied target were on average 3.3 times lower for the lower leg kinematics than for the stance kinetics (Figs. 7 and 8(*a*)). Similarly, there was a lack of significant differences in many kinematic gait parameters, implying that participants in this study walked in such a way as to maintain close-to-able-bodied kinematics regardless of the foot condition they were given. Participants aiming to maintain close-to able-bodied kinematics aligns with the LLTE framework's goal to tune the mechanical characteristics of the prostheses to more closely replicate a target walking pattern, and supports the use of able-bodied kinematics and kinetics as our target walking data in the LLTE framework.

One assumption behind the LLTE framework is that prostheses designed with low LLTE values that enable close replication of the target lower leg dynamics will both be valued by prosthesis users and encourage secondary walking benefits such as increased energy return, reduced trunk sway, or reduced intact limb loading compared to prostheses with high LLTE values [14]. This systematic investigation with varying prosthetic foot stiffness not only showed similar effects on gait dynamics as previous studies [41,42,62–64] but also correlated the beneficial effects with the predicted prosthetic foot LLTE value, with lower LLTE values resulting in prosthetic feet that provide increased walking benefits. A quadratic trend, similar to the one shown in Fig. 8, was also uncovered by Clites et al. [64], experimentally showing that the prosthetic foot with the patient's preferred ankle stiffness maximized ankle kinematic symmetry. Increasing the compliance of prosthetic feet has been shown to enable increased peak push-off power and energy return but at the detriment of a reduced EFLR (which has been linked to knee drop-off effect), increased intact limb loading, and reduced balance [41,42,62,63]. Therefore, there is a tradeoff between providing sufficient compliance to enable increased push-off power and energy return without inducing increased intact limb loading or a drop-off effect at the end of the stance. Here we demonstrate that this tradeoff can be accomplished with the LLTE-optimized stiffness foot, condition C, which achieved similar peak push-off power and returned energy as the most compliant foot conditions while preventing excessive intact limb loading, loss of balance (low trunk sway) or symmetry, or any speed reduction, as well as exhibiting close to able-bodied EFLR and roll-over radius (Table 3).

Despite the extensive information provided by gait studies, many attributes valued by prosthesis users can only be captured through prosthesis evaluation questionnaires [12,55]. In this study, participants' preferences bodied level ground walking aligned with the LLTE value of the prosthetic foot conditions; increased evaluation scores were shown for prosthetic feet with lower LLTE values (Fig. 10). In addition, all participants reported condition C as being the most comfortable prosthesis and the condition they would prefer to use out of all the tested conditions. This suggests that creating prosthetic feet that minimize the LLTE value would provide users with devices that encourage walking benefits and outcomes that are valued by the prosthesis users.

The systematic effects of modifying the LLTE value of a prosthetic foot, and the correlation between the LLTE value and user outcome measures, suggest that this single-value objective could be used to provide insights into the design and development of customized prosthetic feet. Minimizing the LLTE value of a given prosthetic foot design provides a customized and quantitative design process that reduces the need for an iterative design approach and extensive clinical trials. In addition, the LLTE framework is not limited to able-bodied level ground walking but can be applied to any target walking data such as walking on inclines or at varying speeds. The predictive and quantitative capabilities of the LLTE framework would facilitate and streamline the development of prosthetic devices with improved walking performance by reducing the need for clinical trials and design iterations.

The results from this study demonstrate that the LLTE metric is able to differentiate prosthetic feet that resulted in poor replication of the target lower leg dynamics and low participant evaluation scores, such as conditions A and E (high LLTE values) from the foot condition C (the predicted LLTE-optimal condition) that resulted in a close replication of the target lower leg dynamics and high participant evaluation scores (Figs. 7, 8, and 10). However, the results also demonstrate a reduced sensitivity around the LLTE-optimized foot, condition C, with prosthetic foot conditions B and D (±20% of stiffness variation from condition C), resulting in a close replication of the target lower leg dynamics, relatively high participant evaluation scores, and similar walking benefits to condition C. This means that the optimum could be robust to changes in user body mass and walking pattern. The reduced sensitivity around the LLTE-optimized foot also suggests that designers could include additional design objectives such as targeting multiple walking activities or strength constraints without significantly sacrificing walking performance. Similarly, the sensitivity results would enable a comprehensive, quantitative, and discrete sizing of prosthetic feet, similar to a model line of shoes with varying size increments, by creating standardized products. This sizing scheme is especially relevant for prosthetic devices in low and middle-income countries that currently come in a single weight category per foot size. This limits the mobility of users that have the corresponding foot size but a different body mass [13]. Using the LLTE framework, low-cost prosthetic feet could be more easily designed for varying weight categories and foot sizes, improving the mobility of low and middle income countries users.

The correlation and systematic effects of the LLTE value on user walking performance suggest that measuring the LLTE value of existing prosthetic devices using a load testing apparatus could guide the prescription process. The LLTE value would be a unified, single-value measure that would allow for a systematic comparison between commercially available prosthetic foot products. As an amputee-independent measure, the LLTE value could be used as a predictive clinical tool for selecting a reduced set of appropriate prosthetic devices for a specific user and their target walking activity, since prosthetic foot geometries and stiffnesses vary between manufacturers [31].

There are some study limitations to consider when interpreting these results. First, the study included a small participant sample size, which limits the generalization of the results demonstrated here to the overall population of transtibial prosthesis users. There were significant variations among the participants both in terms of their subjective evaluations and their response to variations in prosthetic foot conditions (Fig. 8(*b*)). The effects of changes in LLTE value and prosthetic foot stiffness were more pronounced for participants 3, 4, and 5. Second, the alignment was performed with foot condition C and was kept unchanged for the remaining conditions to avoid confounding factors and only investigate the effect of changes in foot stiffness. The lack of specific alignment for the other conditions could have been the cause of the differences in lower leg dynamics and gait measures. However, for participant 1, the trial period allowed for the collection of two additional trials within the time allocated for the study. The participant walked with foot conditions A and E a second time after the same certified prosthetist specifically aligned each foot condition for the participant. There was no significant change in the measured total lower leg deviation from able-bodied data between the re-aligned conditions and conditions for which the alignment was unchanged from condition C. The fact that similar results and trends were found when re-alignment was performed warranted our decision to maintain the same alignment for all foot conditions. The measured deviations and additional details regarding

these two additional trials are provided in Appendix C. Third, each participant's trial was conducted over a single day with relatively little accommodation time, compared to some studies in which participants had multiple sessions or even weeks to acclimate to a given prosthetic device [65,66]. Nonetheless, our study suggests that participants were able to adapt to the different prosthetic foot conditions, as exhibited by variations in walking patterns between the prostheses. Additional acclimation time might have resulted in larger variations. Fourth, the LLTE framework is currently limited to the sagittal plane; although most kinematic behavior is constrained to this plane [67], a three-dimensional optimization could further improve the performance of LLTE-designed prostheses.

5 Conclusions

In this study, we systematically investigated the effects of varying LLTE values of prosthetic feet on the dynamics of overground transtibial prosthetic gait. For each of the five participants, an LLTE-optimized foot and four additional experimental foot prototypes with varying LLTE values were designed and manufactured. The LLTE values of the foot prototypes were varied by changing the overall stiffness of the LLTE-optimized design by 60%, 80%, 120%, and 167%. Our results suggest that the LLTE values of prosthetic feet are correlated with their ability to enable users to replicate a target walking pattern (kinematics and kinetics), and to user's preferences and clinical outcomes, such as roll-over geometries, trunk sway, prosthetic energy return, and peak push-off power. The prosthetic feet with the lowest LLTE values enabled the closest replication of the target able-bodied walking pattern, encouraged secondary walking benefits, and were preferred by the study participants.

Using the LLTE value as a design objective could streamline the development process of high-performance prosthetic feet. Additionally, measuring the LLTE value of existing prostheses using a load testing apparatus could guide the clinical prescription process. Measuring the LLTE value of existing prostheses would help with selecting a set of appropriate prosthetic devices in terms of stiffness and other mechanical properties for a specific user and target walking profile. This sensitivity study further validates the use of the LLTE framework as a predictive and quantitative tool for designing and evaluating prosthetic feet.

Acknowledgment

The authors would like to thank Rebecca Stine M.S. at the Jesse Brown VA Medical Center for her contribution to participant recruitment and data collection, Martin Buckner, CPO, for fitting and aligning the prostheses, Mr. DR Mehta and Dr. Pooja Mukul at the Jaipur Foot organization (BMVSS) for their continued support and Heidi Peterson and Charlotte Folinus at MIT for their feedback. This work was supported by the Office of the Assistant Secretary of Defense for Health Affairs, through the Peer Reviewed Orthopedic Research Program under Award No. W81XWH-17-1-0427. Opinions, interpretations, conclusions, and recommendations are those of the author and are not necessarily endorsed by the Department of Defense.

Funding Data

- Office of the Assistant Secretary for Health (Funder ID: 10.13039/100006438).

Appendix A: Mechanical Testing of Prosthetic Foot Prototypes

To validate the experimental prototype feet mechanical behaviors, static mechanical tests were conducted using an Instron load testing machine on all the participants' prosthetic foot prototypes. Figure 11 includes the measured displacements of each prototype in response to loading along with the constitutive model results for the remaining four participants.

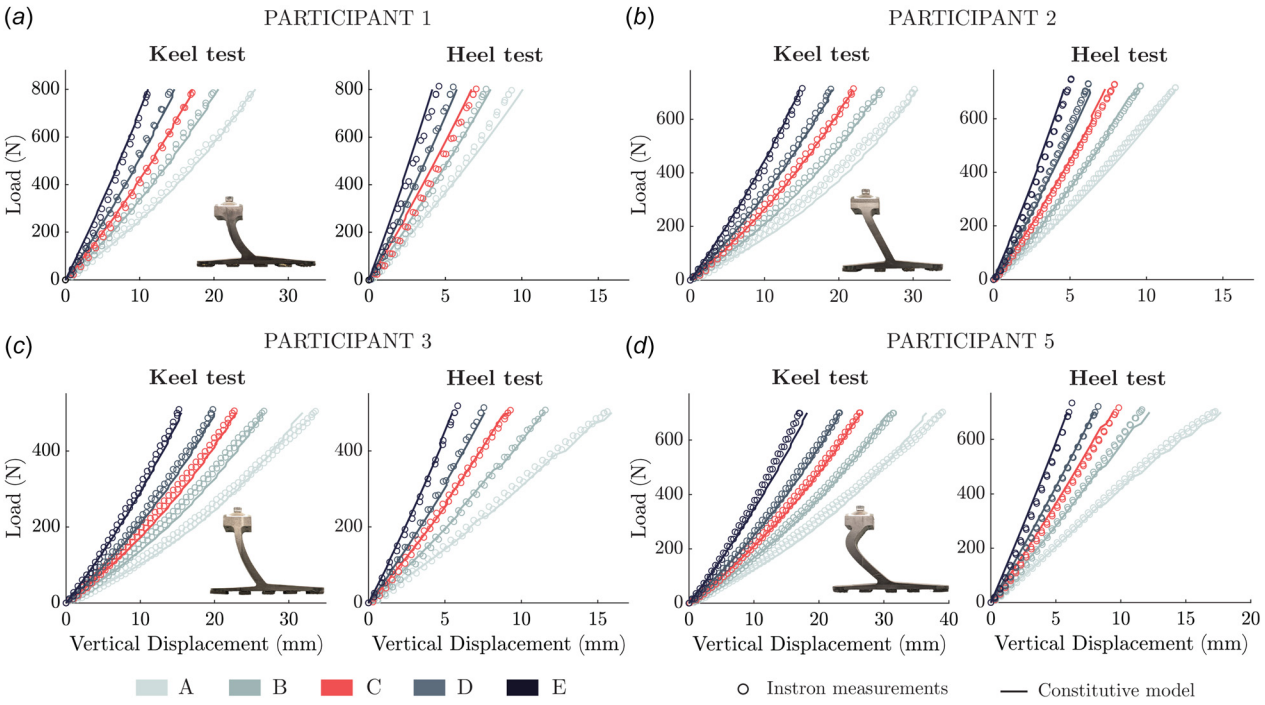

Fig. 11 Load displacement curves for each one of the remaining four participant's five prosthetic foot conditions (A–E) measured with the Instron machine and compare to the constitutive structural model results

Appendix B: GRF Profiles, CoP, and Lower Leg Motion for Each Participant

Individual participant's recorded biomechanical data are included here to complement the participant averaged data presented in Sec. 3.2. For each participant, the kinetic and kinematic variables over the entire stance phase for each prosthetic foot are shown in Figs. 12–16.

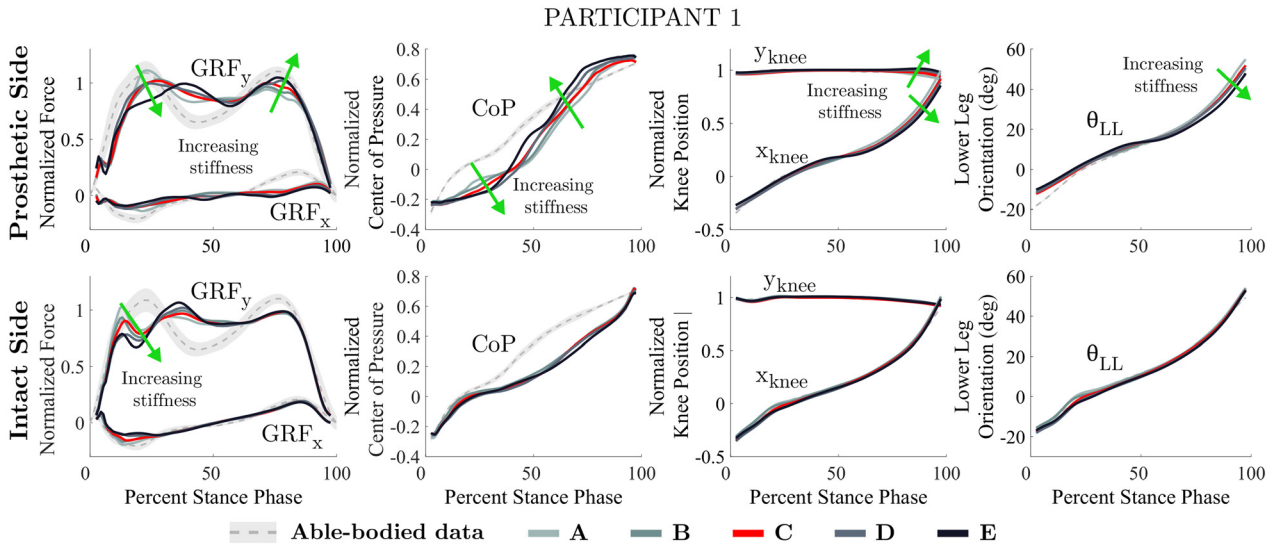

Fig. 12 Average kinetic and kinematic variables over stance phase for participant 1 for each prosthetic foot type averaged across all steps. This includes horizontal and vertical ground reaction forces (GRF_x and GRF_y), center of pressure (CoP) progression, and lower leg position and orientation in the sagittal plane (x_{knee}, y_{knee}, and θ_{LL}) for both the prosthetic and intact side. The shaded regions correspond to one standard deviation of the normative physiological data.

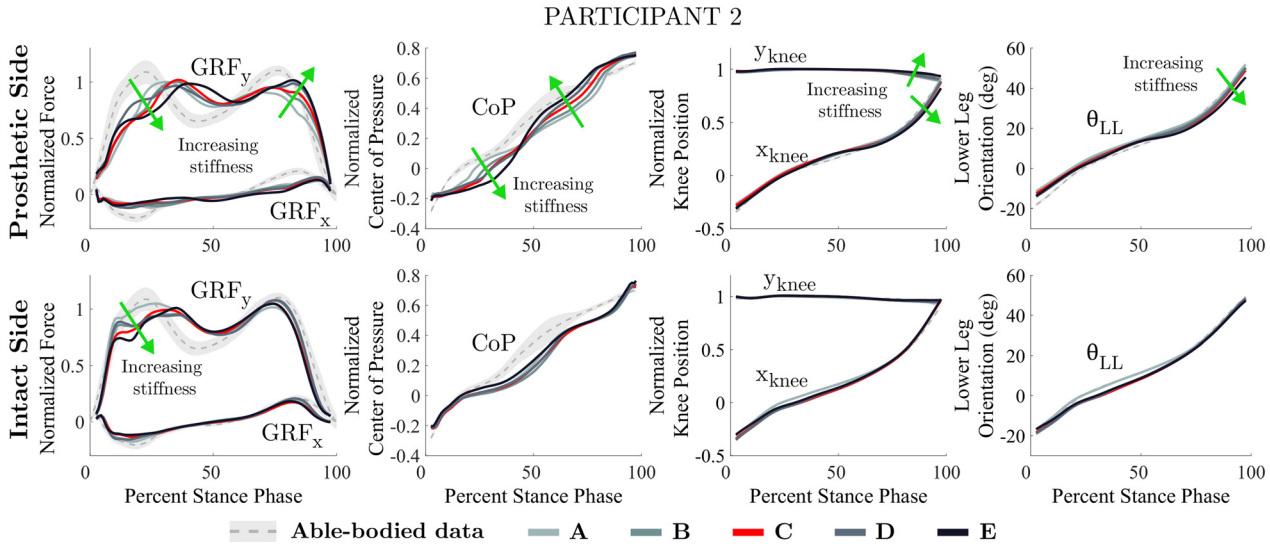

Fig. 13 Average kinetic and kinematic variables over stance phase for participant 2 for each prosthetic foot type averaged across all steps. This includes horizontal and vertical ground reaction forces (GRF_x and GRF_y), center of pressure (CoP) progression, and lower leg position and orientation in the sagittal plane (x_{knee}, y_{knee}, and θ_{LL}) for both the prosthetic and intact side. The shaded regions correspond to one standard deviation of the normative physiological data.

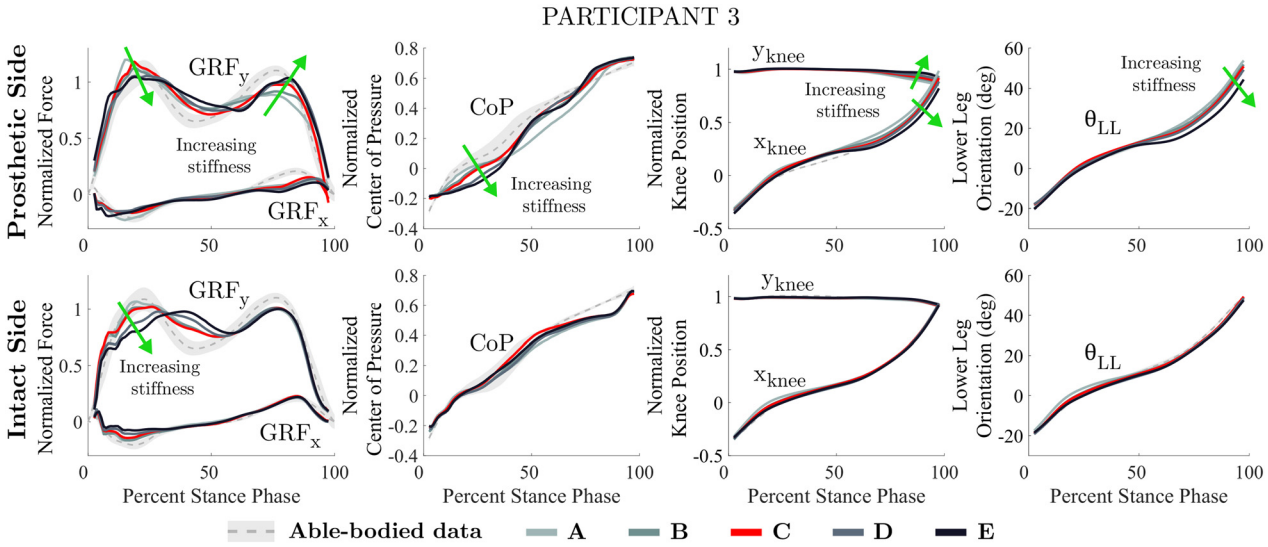

Fig. 14 Average kinetic and kinematic variables over the entire stance phase for participant 3 for each prosthetic foot type averaged across steps. This includes horizontal and vertical ground reaction forces (GRF_x and GRF_y), center of pressure (CoP) progression, and lower leg position and orientation in the sagittal plane (x_{knee}, y_{knee}, and θ_{LL}) for both the prosthetic and intact side. The shaded regions correspond to one standard deviation of the normative physiological data.

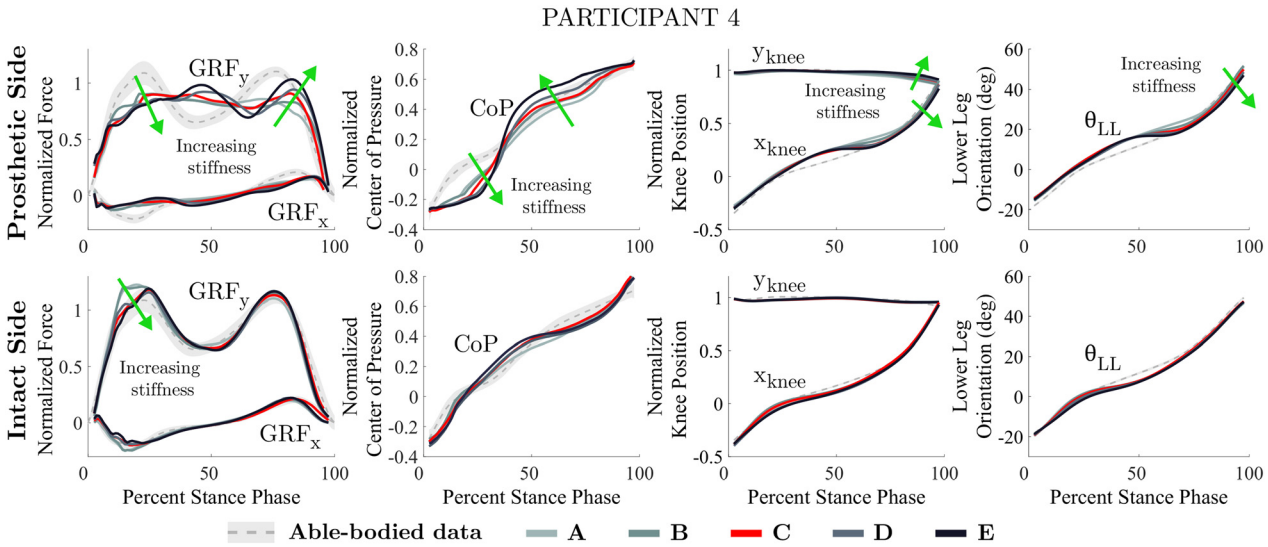

Fig. 15 Average kinetic and kinematic variables over the entire stance phase for participant 4 for each prosthetic foot type averaged across steps. This includes horizontal and vertical ground reaction forces (GRF_x and GRF_y), center of pressure (CoP) progression, and lower leg position and orientation in the sagittal plane (x_{knee}, y_{knee}, and θ_{LL}) for both the prosthetic and intact side. The shaded regions correspond to one standard deviation of the normative physiological data.

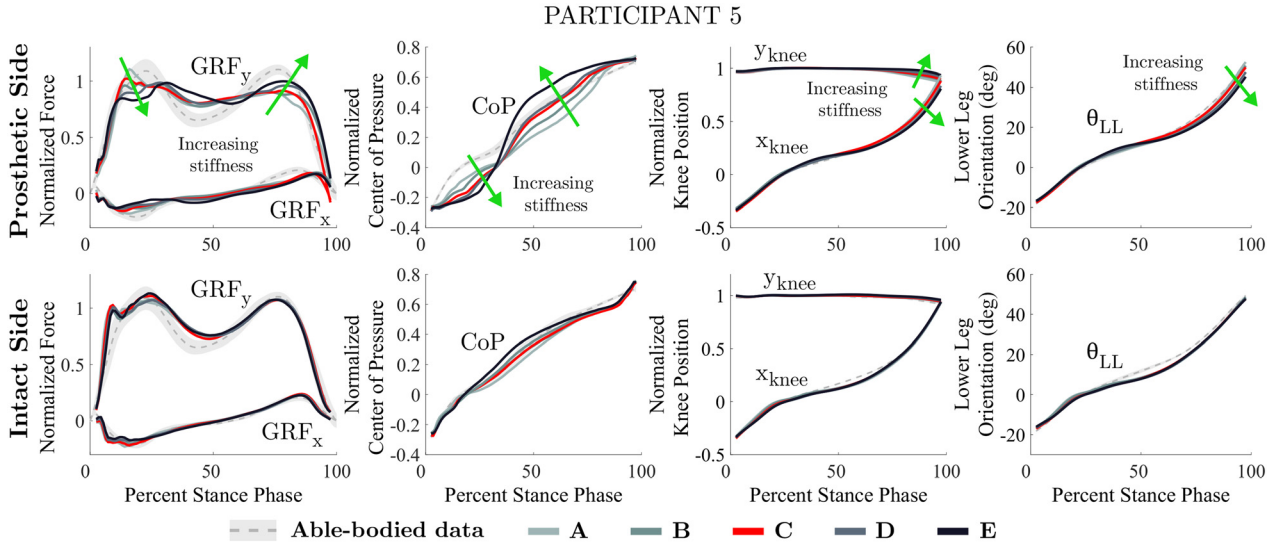

Fig. 16 Average kinetic and kinematic variables over the entire stance phase for participant 5 for each prosthetic foot type averaged across steps. This includes horizontal and vertical ground reaction forces (GRF_x and GRF_y), center of pressure (CoP) progression, and lower leg position and orientation in the sagittal plane (x_{knee}, y_{knee}, and θ_{LL}) for both the prosthetic and intact side. The shaded regions correspond to one standard deviation of the normative physiological data.

Appendix C: Effect of Alignment on Measured Deviation From Target Lower Leg Trajectory

For participant 1, two additional walking trials were collected with conditions A and E, specifically re-aligned by the prosthetist. These trials were conducted to investigate the study decision of keeping the alignment unchanged for all foot conditions. Similarly to the gait study protocol, the participant walked over level ground at their self-selected speeds after a resting and accommodation period with the re-aligned prosthetic foot condition.

The measured lower leg kinematic and kinetic total deviations from the able-bodied target was not different between the trial before and after re-alignment for both condition A and E (Fig. 17). The total deviation for the re-aligned conditions A and E were still significantly higher than the deviations for condition C (single-participant analysis: $p < 0.05$ and $p < 0.05$). These results demonstrated that alignment did not have a significant effect for conditions A and E, and that foot conditions with higher LLTE values still lead to increased deviations compared to conditions with lower LLTE values.

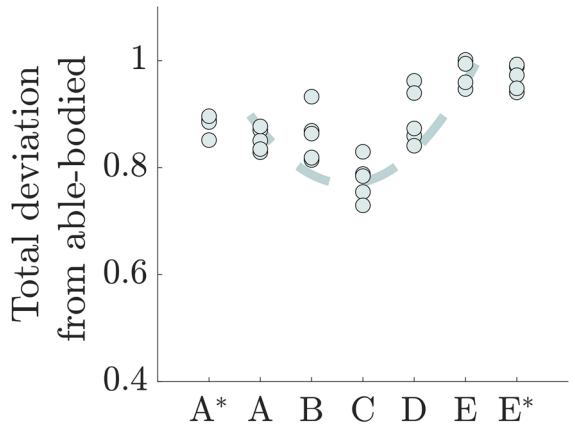

Fig. 17 Measured total deviations from the able-bodied reference data for all prosthetic foot conditions, for participant 1. Foot conditions labeled with * represent conditions for which the prosthetist specifically re-aligned the foot at the start of the walking trial. Total deviation, summed from all six kinematic and kinetic lower leg variables, is shown for each foot condition. Each circular marker represents the total deviation from a single recorded step. The dashed line is the similar quadratic fit of the total deviation from the participant average as shown in Fig. 8.

References

[1] Gailey, R., Allen, K., Castles, J., Kucharik, J., and Roeder, M., 2008, "Review of Secondary Physical Conditions Associated With Lower-Limb Amputation and Long-Term Prosthesis Use," J. Rehabil. Res. Dev., **45**(1), pp. 15–30.

[2] Adamczyk, P. G., and Kuo, A. D., 2015, "Mechanisms of Gait Asymmetry Due to Push-Off Deficiency in Unilateral Amputees," IEEE Trans. Neural Syst. Rehabil. Eng., **23**(5), pp. 776–785.

[3] Major, M. J., and Fey, N. P., 2017, "Considering Passive Mechanical Properties and Patient User Motor Performance in Lower Limb Prosthesis Design Optimization to Enhance Rehabilitation Outcomes," Phys. Ther. Rev., **22**(3–4), pp. 202–216.

[4] Price, M. A., Beckerle, P., and Sup, F. C., 2019, "Design Optimization in Lower Limb Prostheses: A Review," IEEE Trans. Neural Syst. Rehabil. Eng., **27**(8), pp. 1574–1588.

[5] Hafner, B. J., 2005, "Clinical Prescription and Use of Prosthetic Foot and Ankle Mechanisms: A Review of the Literature," J. Prosthet. Orthot., **17**(Suppl), pp. S5–S11.

[6] Major, M. J., Kenney, L. P., Twiste, M., and Howard, D., 2012, "Stance Phase Mechanical Characterization of Transtibial Prostheses Distal to the Socket: A Review," J. Rehabil. Res. Dev., **49**(6), pp. 815–830.

[7] Linde, H. V. D., Hofstad, C. J., Geurts, A. C. H., Postema, K., Geertzen, J. H. B., and van Limbeek, J., 2004, "A Systematic Literature Review of the Effect of Different Prosthetic Components on Human Functioning With a Lower Limb Prosthesis," J. Rehabil. Res. Develop., **41**(4), pp. 555–570.

[8] Hafner, B. J., Sanders, J. E., Czerniecki, J., and Fergason, J., 2002, "Energy Storage and Return Prostheses: Does Patient Perception Correlate With Biomechanical Analysis?," Clinical Biomech., **17**(5), pp. 325–344.

[9] Raschke, S. U., Orendurff, M. S., Mattie, J. L., Kenyon, D. E., Jones, O. Y., Moe, D., Winder, L., Wong, A. S., Moreno-Hernández, A., Highsmith, M. J., Sanderson, D. J., and Kobayashi, T., 2015, "Biomechanical Characteristics, Patient Preference and Activity Level With Different Prosthetic Feet: A Randomized Double Blind Trial With Laboratory and Community Testing," J. Biomech., **48**(1), pp. 146–152.

[10] Hofstad, C. J., Linde, H., Limbeek, J., and Postema, K., Cochrane Bone, Joint and Muscle Trauma Group 2004, "Prescription of Prosthetic Ankle-Foot Mechanisms After Lower Limb Amputation," Cochrane Database Syst. Rev., **2010**(1), p. CD003978.

[11] Kaufman, K. R., and Bernhardt, K., 2021, "Functional Performance Differences Between Carbon Fiber and Fiberglass Prosthetic Feet," Prosthetics Orthotics Int., **45**(3), pp. 205–213.

[12] Schaffalitzky, E., Gallagher, P., MacLachlan, M., and Wegener, S. T., 2012, "Developing Consensus on Important Factors Associated With Lower Limb Prosthetic Prescription and Use," Disabil. Rehabil., **34**(24), pp. 2085–2094.

[13] Laferrier, J. Z., Groff, A., Hale, S., and Sprunger, N. A., 2018, "A Review of Commonly Used Prosthetic Feet for Developing Countries: A Call for Research and Development," J. Nov. Physiother., **08**(01), pp. 1–10.

[14] Olesnavage, K. M., and Winter, A. G., 2018, "A Novel Framework for Quantitatively Connecting the Mechanical Design of Passive Prosthetic Feet to Lower Leg Trajectory," IEEE Trans. Neural Syst. Rehabil. Eng., **26**(8), pp. 1544–1555.
[15] Prost, V., Johnson, W. B., Kent, J. A., Major, M. J., and Winter, A. G., 2022, "Biomechanical Evaluation Over Level Ground Walking of User-Specific Prosthetic Feet Designed Using the Lower Leg Trajectory Error Framework," Sci. Rep., **12**(1), pp. 1–15.
[16] Witte, K. A., Fiers, P., Sheets-Singer, A. L., and Collins, S. H., 2020, "Improving the Energy Economy of Human Running With Powered and Unpowered Ankle Exoskeleton Assistance," Sci. Rob., **5**(40), p. eaay9108.
[17] Czerniecki, J. M., and Morgenroth, D. C., 2017, "Metabolic Energy Expenditure of Ambulation in Lower Extremity Amputees: What Have we Learned and What Are the Next Steps?," Disabil. Rehabil., **39**(2), pp. 143–151.
[18] Welker, C. G., Voloshina, A. S., Chiu, V. L., and Collins, S. H., 2021, "Shortcomings of Human-in-the-Loop Optimization of an Ankle-Foot Prosthesis Emulator: A Case Series," R. Soc. Open Sci., **8**(5), p. 202020.
[19] Hedrick, E. A., Stanhope, S. J., and Takahashi, K. Z., 2019, "The Foot and Ankle Structures Reveal Emergent Properties Analogous to Passive Springs During Human Walking," PLoS ONE, **14**(6), p. e0218047.
[20] Pollen, T., 2015, "A Non-Biomimetic Approach For Producing Shank Kinematics And Energetics," Ph.D. thesis, University of Delaware, ProQuest Dissertations, Ann Arbor, MI.
[21] Kolbeinsdóttir, R., 2018, "Shank Kinematics and Kinetics in Prosthetic Gait: Implications for Improved Design of Prosthetic Systems," Ph.D. thesis, University of Delaware, ProQuest Dissertations, Ann Arbor, MI.
[22] Olesnavage, K. M., Prost, V., Johnson, W. B., and Amos Winter, V. G., 2018, "Passive Prosthetic Foot Shape and Size Optimization Using Lower Leg Trajectory Error," ASME J. Mech. Des., **140**(10), p. 102302.
[23] Prost, V., Olesnavage, K. M., Johnson, W. B., Major, M. J., and Winter, V. A. G., 2018, "Design and Testing of a Prosthetic Foot With Interchangeable Custom Springs for Evaluating Lower Leg Trajectory Error, an Optimization Metric for Prosthetic Feet," ASME J. Mechanisms Robotics, **10**(2), p. 021010.
[24] Olesnavage, K., Prost, V., Johnson, B., Major, M., and Winter, A. G., 2021, "Experimental Demonstration of the Lower Leg Trajectory Error Framework Using Physiological Data as Input," ASME J. Biomech. Eng., **143**(3), p. 031003.
[25] Prost, V., Peterson, H. P., and Winter, A. G., 2023, "Multi-Keel Passive Prosthetic Foot Design Optimization Using the Lower Leg Trajectory Error Framework," ASME J. Mechanisms Robotics, **15**(4), p. 041001.
[26] Prost, V., 2021, "Development and Validation of a Passive Prosthetic Foot Design Framework based on Lower Leg Dynamics," Ph.D. dissertation, Massachusetts Institute of Technology, Cambridge, MA.
[27] Johnson, W. B., Prost, V., Mukul, P., and Winter, V. A. G., 2023, "Design and Evaluation of High-Performance, Low-Cost Prosthetic Feet for Developing Countries," ASME J. Med. Devices, **17**(1), p. 011003.
[28] Winter, D. A., 2009, *Biomechanics and Motor Control of Human Movement*, 4th ed., John Wiley & Sons, Hoboken, NJ.
[29] Shepherd, M. K., Azocar, A. F., Major, M. J., and Rouse, E. J., 2018, "Amputee Perception of Prosthetic Ankle Stiffness During Locomotion," J. NeuroEng. Rehabil., **15**(1), pp. 1–10.
[30] Huston, C., Dillingham, T. R., and Esquenazi, A., 1998, "Rehabilitation of the Lower Limb Amputee," Rehabilitation Injured Combatant, Office of The Surgeon General Department of the Army, United States of America, Washington, DC, Vol. 1, pp. 79–159.
[31] Webber, C. M., and Kaufman, K., 2017, "Instantaneous Stiffness and Hysteresis of Dynamic Elastic Response Prosthetic Feet," Prosthet. Orthot. Int., **41**(5), pp. 463–468.
[32] Shepherd, M. K., and Rouse, E. J., 2020, "Comparing Preference of Ankle-Foot Stiffness in Below-Knee Amputees and Prosthetists," Sci. Rep., **10**(1), pp. 1–8.
[33] Gailey, R. S., Nash, M. S., Atchley, T. A., Zilmer, R. M., Moline-Little, G. R., Morris-Cresswell, N., and Siebert, L. I., 1997, "The Effects of Prosthesis Mass on Metabolic Cost of Ambulation in Non-Vascular Trans-Tibial Amputees," Prosthet. Orthot. Int., **21**(1), pp. 9–16.
[34] Selles, R. W., Bussmann, J. B., Van Soest, A. J., and Stam, H. J., 2004, "The Effect of Prosthetic Mass Properties on the Gait of Transtibial amputees - A Mathematical Model," Disabil. Rehabil., **26**(12), pp. 694–704.
[35] Kadaba, M. P., Ramakrishnan, H. K., Wootten, M. E., Gainey, J., Gorton, G., and Cochran, G. V. B., 1989, "Repeatability of Kinematic, Kinetic, and Electromyographic Data in Normal Adult Gait," J. Orthop. Res., **7**(6), pp. 849–860.
[36] Major, M. J., Scham, J., and Orendurff, M., 2018, "The Effects of Common Footwear on Stance-Phase Mechanical Properties of the Prosthetic Foot-Shoe System," Prosthet. Orthot. Int., **42**(2), pp. 198–207.
[37] Hansen, A. H., Childress, D. S., and Knox, E. H., 2000, "Prosthetic Foot Roll-Over Shapes With Implications for Alignment of Trans-Tibial Prostheses," Prosthet. Orthot. Int., **24**(3), pp. 205–215.
[38] Kadaba, M. P., Ramakrishnan, H. K., and Wootten, M. E., 1990, "Measurement of Lower-Extremity Kinematics During Level Walking," J. Orthop. Res., **8**(3), pp. 383–392.
[39] Kent, J. A., Arelekatti, V. M., Petelina, N. T., Johnson, W. B., Brinkmann, J. T., Winter, A. G., and Major, M. J., 2021, "Knee Swing Phase Flexion Resistance Affects Several Key Features of Leg Swing Important to Safe Transfemoral Prosthetic Gait," IEEE Trans. Neural Syst. Rehabil. Eng., **29**, pp. 965–973.
[40] Pinzone, O., Schwartz, M. H., and Baker, R., 2016, "Comprehensive Non-Dimensional Normalization of Gait Data," Gait Posture, **44**, pp. 68–73.
[41] Fey, N. P., Klute, G. K., and Neptune, R. R., 2011, "The Influence of Energy Storage and Return Foot Stiffness on Walking Mechanics and Muscle Activity in Below-Knee Amputees," Clinical Biomech., **26**(10), pp. 1025–1032.
[42] Klodd, E., Hansen, A., Fatone, S., and Edwards, M., 2010, "Effects of Prosthetic Foot Forefoot Flexibility on Gait of Unilateral Transtibial Prosthesis Users," J. Rehabil. Res. Dev., **47**(9), pp. 899–910.
[43] Adamczyk, P. G., and Kuo, A. D., 2013, "Mechanical and Energetic Consequences of Rolling Foot Shape in Human Walking," J. Exp. Biol., **216**(Pt 14), pp. 2722–2731.
[44] Crimin, A., McGarry, A., Harris, E. J., and Solomonidis, S. E., 2014, "The Effect That Energy Storage and Return Feet Have on the Propulsion of the Body: A Pilot Study," J. Eng. Med., **228**(9), pp. 908–915.
[45] Alexander, R., 1989, "Optimization and Gaits in the Locomotion of Vertebrates," Physiol. Rev., **69**(4), pp. 1199–1227.
[46] Robinson, R., Herzog, W., and Nigg, B. M., 1987, "Use of Force Platform Variables to Quantify the Effects of Chiropractic Manipulation on Gait Symmetry," J. Manipulative Physiol. Ther., **10**(4), pp. 172–176.
[47] Gates, D. H., Scott, S. J., Wilken, J. M., and Dingwell, J. B., 2013, "Frontal Plane Dynamic Margins of Stability in Individuals With and Without Transtibial Amputation Walking on a Loose Rock Surface," Gait Posture, **38**(4), pp. 570–575.
[48] Major, M. J., Stine, R. L., and Gard, S. A., 2013, "The Effects of Walking Speed and Prosthetic Ankle Adapters on Upper Extremity Dynamics and Stability-Related Parameters in Bilateral Transtibial Amputee Gait," Gait Posture, **38**(4), pp. 858–863.
[49] Sawers, A., and Hahn, M. E., 2011, "Trajectory of the Center of Rotation in Non-Articulated Energy Storage and Return Prosthetic Feet," J. Biomech., **44**(9), pp. 1673–1677.
[50] Hansen, A. H., Childress, D. S., Miff, S. C., Gard, S. A., and Mesplay, K. P., 2004, "The Human Ankle During Walking: Implications for Design of Biomimetic Ankle Prostheses," J. Biomech., **37**(10), pp. 1467–1474.
[51] Takahashi, K. Z., Kepple, T. M., and Stanhope, S. J., 2012, "A Unified Deformable (UD) Segment Model for Quantifying Total Power of Anatomical and Prosthetic Below-Knee Structures During Stance in Gait," J. Biomech., **45**(15), pp. 2662–2667.
[52] Zelik, K. E., and Honert, E. C., 2018, "Ankle and Foot Power in Gait Analysis: Implications for Science, Technology and Clinical Assessment," J. Biomech., **75**, pp. 1–12.
[53] Esposito, E. R., Whitehead, J. M., and Wilken, J. M., 2016, "Step-to-Step Transition Work During Level and Inclined Walking Using Passive and Powered Ankle-Foot Prostheses," Prosthet. Orthot. Int., **40**(3), pp. 311–319.
[54] Donelan, J. M., Kram, R., and Kuo, A. D., 2002, "Simultaneous Positive and Negative External Mechanical Work in Human Walking," J. Biomech., **35**(1), pp. 117–124.
[55] Baars, E. C., Schrier, E., DIjkstra, P. U., and Geertzen, J. H., 2018, "Prosthesis Satisfaction in Lower Limb Amputees: A Systematic Review of Associated Factors and Questionnaires," Medicine, **97**(39), p. e12296.
[56] Harry, J., Eggleston, J., Lidstone, D., and Dufek, J., 2019, "Weighted Vest Use to Improve Movement Control During Walking in Children With Autism," Transl. J. Am. Coll. Sports Med., **4**(10), pp. 64–73.
[57] Bates, B., James, C., and Dufek, J., 2004, "Single-Subject Analysis," Innovative Analyses Human Movement, Human Kinetics, Champaign, IL, pp. 3–28.
[58] Hansen, A. H., Sam, M., and Childress, D. S., 2004, "The Effective Foot Length Ratio: A Potential Tool for Characterization and Evaluation of Prosthetic Feet," J. Prosthet. Orthot., **16**(2), pp. 41–45.
[59] Houdijk, H., Pollmann, E., Groenewold, M., Wiggerts, H., and Polomski, W., 2009, "The Energy Cost for the Step-to-Step Transition in Amputee Walking," Gait Posture, **30**(1), pp. 35–40.
[60] Morgenroth, D. C., Segal, A. D., Zelik, K. E., Czerniecki, J. M., Klute, G. K., Adamczyk, P. G., Orendurff, M. S., Hahn, M. E., Collins, S. H., and Kuo, A. D., 2011, "The Effect of Prosthetic Foot Push-Off on Mechanical Loading Associated With Knee Osteoarthritis in Lower Extremity Amputees," Gait Posture, **34**(4), pp. 502–507.
[61] Farrokhi, S., Mazzone, B., Yoder, A., Grant, K., and Wyatt, M., 2016, "A Narrative Review of the Prevalence and Risk Factors Associated With Development of Knee Osteoarthritis After Traumatic Unilateral Lower Limb Amputation," Military Med., **181**(S4), pp. 38–44.
[62] Adamczyk, P. G., Collins, S. H., and Kuo, A. D., 2006, "The Advantages of a Rolling Foot in Human Walking," J. Exp. Biol., **209**(20), pp. 3953–3963.
[63] Hansen, A. H., Meier, M. R., Sessoms, P. H., and Childress, D. S., 2006, "The Effects of Prosthetic Foot Roll-Over Shape Arc Length on the Gait of Trans-Tibial Prosthesis Users," Prosthet. Orthot. Int., **30**(3), pp. 286–299.
[64] Clites, T. R., Shepherd, M. K., Ingraham, K. A., Wontorcik, L., and Rouse, E. J., 2021, "Understanding Patient Preference in Prosthetic Ankle Stiffness," J. NeuroEng. Rehabil., **18**(1), pp. 1–16.
[65] Zhang, X., Fiedler, G., and Liu, Z., 2019, "Evaluation of Gait Variable Change Over Time as Transtibial Amputees Adapt to a New Prosthesis Foot," BioMed Res. Int., **2019**(i), pp. 1–6.
[66] Wanamaker, A. B., Andridge, R. R., and Chaudhari, A. M., 2017, "When to Biomechanically Examine a Lower-Limb Amputee: A Systematic Review of Accommodation Times," Prosthet. Orthot. Int., **41**(5), pp. 431–445.
[67] Fey, N. P., Klute, G. K., and Neptune, R. R., 2013, "Altering Prosthetic Foot Stiffness Influences Foot and Muscle Function During Below-Knee Amputee Walking: A Modeling and Simulation Analysis," J. Biomech., **46**(4), pp. 637–644.